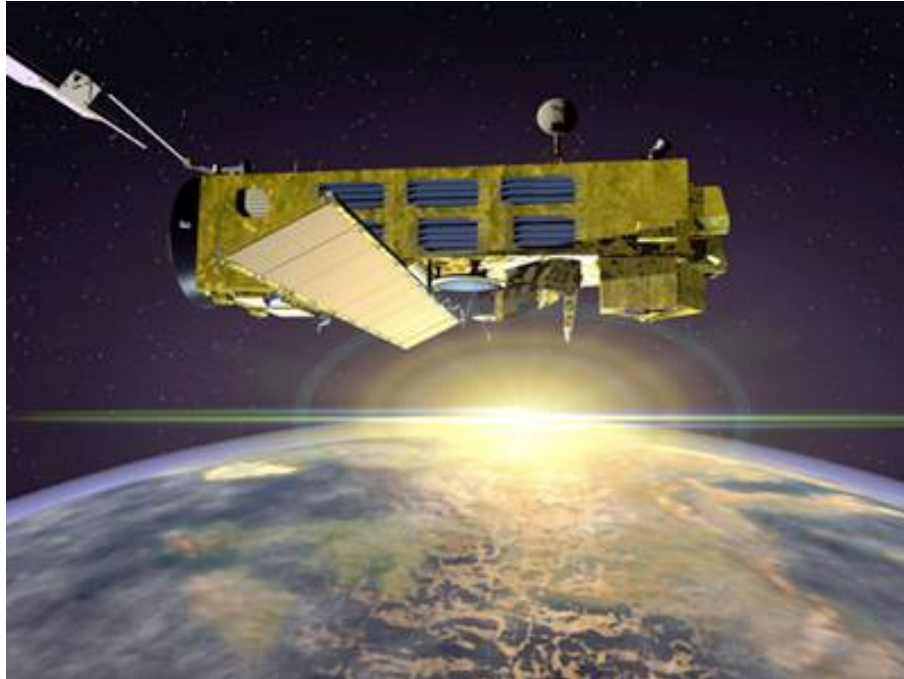


---

## ENVISAT GOMOS report: October 2008



---

Prepared by:	L. Saavedra de Miguel - SERCO
Approved by:	Angelika Dehn - SERCO
Inputs from:	GOMOS Quality Working Group, ECMWF
Issue:	1.0
Reference:	ENVI-SPPA-EOPG-TN-08-0054
Date of issue:	10 <sup>th</sup> November 2008
Status:	Reviewed
Document type:	Technical Note

# T A B L E O F C O N T E N T S

<b>1 INTRODUCTION.....</b>	<b>3</b>
1.1 Scope .....	3
1.2 References.....	3
1.3 Acronyms and Abbreviations.....	4
<b>2 SUMMARY .....</b>	<b>6</b>
<b>3 INSTRUMENT AND DATA AVAILABILITY.....</b>	<b>7</b>
3.1 GOMOS Unavailability Periods .....	7
3.2 Stars Lost in Centering.....	8
3.3 Stars lost due to VCCS anomaly.....	10
3.4 Data Generation Gaps.....	10
3.5 Data availability to users.....	11
<b>4 INSTRUMENT CONFIGURATION AND PERFORMANCE.....</b>	<b>12</b>
4.1 Instrument Operation and Configuration.....	12
4.1.1 Operations since beginning of mission .....	12
4.1.2 Current operations and configuration.....	14
4.2 Limb, Illumination conditions and instrument gain setting.....	15
4.3 Thermal Performance.....	16
4.4 Optomechanical Performance.....	20
4.5 Electronic Performance.....	21
4.5.1 Dark Charge Evolution and Trend.....	21
4.5.2 Signal Modulation .....	24
4.5.3 Electronic Chain Gain and Offset.....	24
4.6 Acquisition, Detection and Pointing Performance.....	25
4.6.1 SATU Noise Equivalent Angle .....	25
4.6.2 Tracking Loss Information.....	27
4.6.3 Most Illuminated Pixel (MIP).....	30
<b>5 LEVEL 1 PRODUCT QUALITY MONITORING .....</b>	<b>31</b>
5.1 Processor Configuration.....	31
5.1.1 Version.....	31
5.1.2 Auxiliary Data files (ADF).....	34
5.2 Quality Flags Monitoring.....	37
5.2.1 Quality Flags Monitoring (extracted from Level 2 products).....	39
5.3 Spectral Performance.....	43
5.4 Radiometric Performance.....	44
5.4.1 Radiometric Sensitivity.....	44
5.4.2 Pixel Response Non Uniformity.....	45
5.5 Other Calibration Results.....	45
<b>6 LEVEL 2 PRODUCT QUALITY MONITORING .....</b>	<b>46</b>
6.1 Processor Configuration.....	46
6.1.1 Version.....	46
6.1.2 Auxiliary Data Files (ADF).....	48
6.1.3 Re-Processing Status.....	49
6.2 Quality Flags Monitoring.....	49
6.3 Other Level 2 Performance Issues .....	51
6.3.1 Monthly Ozone average.....	51
6.3.2 Ozone dispersion monitoring .....	52

**7 VALIDATION ACTIVITIES AND RESULTS ..... 54**

7.1 GOMOS-ECMWF Comparisons (Rossana Dragani, ECMWF input) ..... 54

7.2 Comparison of ozone and temperature profiles with lidar data - Satellite validation with lidar (VALID) (A. van Gijssel, RIVM, QWG input)..... 55

# 1 INTRODUCTION

The GOMOS monthly report documents the current status and recent changes to the GOMOS instrument, its data processing chain, and its data products.

The Monthly Report (hereafter MR) is composed of analysis results obtained by the Data Processing and Quality Control, combined with inputs received from the different entities working on GOMOS operation, calibration, product validation and data quality. These teams participate in the GOMOS Quality Working Group:

- European Space Agency (ESRIN, ESOC, ESTEC-PLSO)
- IDEAS
- ACRI
- Service d'Aeronomie
- Finnish Meteorological Institute
- IASB-Belgian Institute for Space Aeronomy
- Astrium Space
- ECMWF

In addition, the group interfaces with the Atmospheric Chemistry Validation Team.

## 1.1 *Scope*

The main objective of the Monthly Report is to give, on a regular basis, the status of GOMOS instrument performance, data acquisition, results of anomaly investigations, calibration activities and validation campaigns. The following six sections compose the MR:

- Summary
- Unavailability
- Instrument Configuration and Performance
- Level 1 Product Quality Monitoring
- Level 2 Product Quality Monitoring
- Validation Activities and Results

## 1.2 *References*

- [1] ENVISAT Weekly Mission Operations Report #326, #327, #328 and #329
- [2] ECMWF GOMOS Monthly Reports
- [3] Routine update of the wavelength assignment, Gilbert Barrot (ACRI-ST), Issue 1 Revision 1, September 19, 2007
- [4] H. Nazaryan, M.P. McCormick, and J.M. Russell III, Comparative analysis of SBUV/2 and HALOE ozone profiles and trends, JGR, vol. 112, D10304, doi: 10.1029/2006JD007367, 2007.
- [5] A.E. van Gijsel and D.P.J. Swart, GOMOS 6.0cf and 7.0ab comparison with lidar, sonde and microwave radiometer data, VALID report September 2008.

### 1.3 *Acronyms and Abbreviations*

ACVT	Atmospheric Chemistry Validation Team
ADC	Analogue-to-Digital Converter
ADF	Auxiliary Data File
ADS	Auxiliary Data Server
ANX	Ascending Node Crossing
AOCS	Attitude and Orbit Control System
ARB	Anomaly Review Board
ARF	Archiving Facility (PDS)
CCU	Central Communication Unit
CFS	CCU Flight Software
CNES	Centre National d'Études Spatiales
CTI	Configuration Table Interface / Configurable Transfer Item
CR	Cyclic Report
DC	Dark Charge
DMOP	Detailed Mission Operation Plan
DPM	Detailed Processing Model
DS	Data Server
DSA	Dark Sky Area
DSD	Data Set Descriptor
ECMWF	European Centre for Medium Weather Forecast\
EO	Earth Observation
EQSOL	Equipment Switch Off Line
ESA	European Space Agency
ESL	Expert Support Laboratory
ESRIN	European Space Research Institute
ESTEC	European Space Research & Technology Centre
ESOC	European Space Operations Centre
FCM	Fine Control Mode
FinCoPAC	Finnish Products Archiving Center
FMI	Finnish Meteorological Institute
FOCC	Flight Operations Control Centre (ENVISAT)
FP1	Fast Photometer 1
FP2	Fast Photometer 2
GADS	Global Annotations Data Set
GOMOS	Global Ozone Monitoring by Occultation of Stars
GOPR	Gomos Prototype
GS	Ground Segment
HK	Housekeeping
IASB	Institut d'Aeronomie Spatiale de Belgique
IAT	Interactive Analysis Tool
ICU	Instrument Control Unit
IDEAS	Instrument Data quality Evaluation and Analysis
IDL	Interactive Data Language
IECF	Instrument Engineering and Calibration Facilities
IMK	Institute of Meteorology Karlsruhe (Meteorologisch Institut Karlsruhe)
INV	Inventory Facilities (PDS)

IPF	Instrument Processing Facilities (PDS)
JPL	Jet Propulsion Laboratory
LAN	Local Area Network
LMA	Levenberg-Marquardt Algorithm
LPCE	Laboratoire de Physique et Chimie de l'Environnement
LRAC	Low Rate Archiving Center
LUT	Look Up Table
MCMD	Macro Command
MDE	Mechanism Drive Electronics
MIP	Most Illuminated Pixel
MPH	Main Product Header
MPS	Mission Planning System
MR	Monthly Report
NRT	Near Real Time
OBDH	On-Board Data Handling
OBT	On Board Time
OCM	Orbit Control Manoeuvre
OOP	Out-of-plane
OP	Operational Phase of ENVISAT
PAC	Processing and Archiving Centre (PDS)
PCF	Product Control Facility
PDCC	Payload Data Control Centre (PDS)
PDHS	Payload Data Handling Station (PDS)
PDHS-E	Payload Data Handling Station – ESRIN
PDHS-K	Payload Data Handling Station – Kiruna
PDS	Payload Data Segment
PEB	Payload Equipment Bay
PLSOL	Payload Switch off Line
PMC	Payload Module Computer
PRNU	Pixel Response Non Uniformity
PSO	On-Orbit Position
QC	Quality Control
QUARC	Quality Analysis and Reporting Computer
QWG	Quality Working Group
RDV	RenDez-Vous
RGT	ROP Generation Tool
RIVM	Rijksinstituut voor Volksgezondheid en Milieu
ROP	Reference Operations Plan
RRM	Rate Reduction Mode
RTS	Random Telegraphic Signal
SA	Service d'Aeronomie
SAA	South Atlantic Anomaly
SATU	Star Acquisition and Tracking Unit
SFA	Steering Front Assembly
SFCM	Stellar Fine Control Mode
SFM	Steering Front Mechanism
SM	Service Module
SMNA	Servicio Meteorológico Nacional de Argentina

SMP	Set Measurement Parameter
SODAP	Switch On and Data Acquisition Phase
SPA1	Spectrometer A CCD 1
SPA2	Spectrometer A CCD 2
SPB1	Spectrometer B CCD 1
SPB2	Spectrometer B CCD 2
SPH	Specific Product Header
SQADS	Summary Quality Annotation Data Set
SSP	Sun Shade Position
STP	Set Thermal Parameter
SYSTEM	Stellar Yaw Steering Mode
SZA	Solar Zenith Angle
VCCS	Voice Coil Command Saturation

## 2 SUMMARY

**Instrument availability** (section 3.1): There were no unavailability periods during the reporting period.

**Instrument operations** (section 4.1.2): The instrument was operating with a reduced azimuth window of 30° (since 2<sup>nd</sup> February 2008) and a minimum allowed azimuth angle set to +2°. These two restrictions in azimuth are aimed to avoid any the Voice Coil Command Saturation anomaly which could stress the mechanism.

**Voice-Coil Command Saturation (VCCS) Anomaly** (section 3.3): No VCCS anomaly occurred during nominal operations.

**Data availability** when instrument was in operation (section 3.4): During the reporting period the availability of Level 0 and Level 1 NRT was higher than 99%.

**Data availability for users** (section 3.5): Routine dissemination of Level 1b and Level 2 products produced by the PDS to the users is enabled. Level 1b data are available on request to the EO Helpdesk ([EOHelp@esa.int](mailto:EOHelp@esa.int)), while level 2 data are available for the whole mission on different ftp sites. All data (reprocessed, NRT and consolidated) are processed with the same version of GOMOS processor.

**Wavelength monitoring** (section 5.3): This month, as in the previous one, the wavelength shifts are higher than 0.08 nm (threshold is 0.07 nm) which is something not expected after the implementation of the routine calibration on 14<sup>th</sup> December 2007. The QWG has been informed and is investigating this issue.

**Pointing performance** (section 4.6.1): the SATU NEA ('Y' axis) had a gradual increase since mid April 2006 until October 2007. This increase was due to fluctuations of the SATU 'Y' data observed at the beginning of nominal occultations (starting at 130 km that corresponds to an elevation angle of around 65°). Preliminary investigations carried out by the ESL, ESA and industry pointed to a problem on the SFM (mechanical or electrical) and not to a problem on the SATU itself. Since November 2007 no fluctuations have been observed and the daily SATU 'Y' average has come back below the threshold set to 3 micro radians.

**Temperatures** (section 4.3): The CCD temperatures show the expected global increase due to the radiator ageing. Another expected variation of the temperatures, the seasonal one, with amplitude of around 1.5 degree can also be observed.

**Modulation signal** (section 4.5.2): The values of the modulation are daily extracted and plotted; they should not be very different from the ones coded into the processor: 1.40 ADU for SPA1 and 0.76 ADU for SPA2. The modulation signal shows high values during summer time for the ESRIN data, it now being confirmed that the South Atlantic Anomaly is the cause of these unexpected peaks. The quality of ESRIN data, in particular over the SAA zone, is impacted but the measure of this impact is under investigation. However, in the second half of the months of October of all years (2004-2007) the peaks are smaller because the DSA zone where the data are taken for this analysis is moving towards the Northern Hemisphere. At the end of October the DSA zone is definitely chosen by the planning system in the Northern Hemisphere (to fill the criteria ‘DSA in full dark limb conditions’) and the high peaks disappear.

**Star detection performance** (section 4.6.3): the stars should be detected not far from the SATU center, that is, pixel number 145 in elevation and number 205 in azimuth. The elevation MIP (Most Illuminated Pixel, which is the pixel at the moment of the detection) had a significant variation until 12<sup>th</sup> December 2003 when a new PSO algorithm was activated in order to reduce the deviations of the ENVISAT platform attitude with respect to the nominal one. Afterwards, the MIP position was quite stable around its nominal pixel values until the occurrence of the VCCS anomaly on January 2005. The reason for the change in trend observed after the anomaly is, at the moment, not understood. This behavior, currently stable at pixel 127 in elevation and 193 in azimuth, does not impact the data quality but may invalidate attitude monitoring by GOMOS and could represent a hidden anomaly.

**Radiometric sensitivity monitoring** (section 5.4.1): for stars 25 and 9, the UV ratio is greater than the threshold 10%. It is clear that there is a global decrease of UV ratios for all the stars. This confirms the expected degradation suffered by the UV optics that is, anyway, very small considering also the small variation for the rest of the stars. For the photometers radiometric sensitivity ratios it is observed that every star has a variation that seems to be seasonally related. The variation is significant for stars 25 and 18. After some investigations performed by the QWG that exclude an inaccurate reflectivity correction LUT, it seems that the PH1/2 radiometric sensitivity variations could come from the fact that the spectrometers and the photometers are not illuminated the same way when the straylight appears.

**Auxiliary Data File** (sections 5.1.2 and 5.3): Three GOM\_CAL\_AX files with updated DC maps and new wavelength assignment have been disseminated during the reporting period.

## 3 INSTRUMENT AND DATA AVAILABILITY

### 3.1 *GOMOS Unavailability Periods*

There were no unavailability periods during the reporting month.



**Table 3-1: List of unavailability periods issued during the reporting month**

Reference of unavailability report	Start time Star orbit	Stop time Stop orbit	Description
-	-	-	-

### 3.2 *Stars Lost in Centering*

The acquisition of a star initiates with a rallying phase where the telescope mechanism is directed towards the expected position of the star. Subsequently the acquisition procedure enters into detection mode, where the SATU star tracker output signal is pre-processed for spot presence survey and for the location of the most illuminated couple of adjacent pixels for two added lines, over the detection field. The Most Illuminated Pixel (MIP) defines the position of the first SATU centering window. The following step in the acquisition sequence is then initiated and consists of a centering phase where the SATU output signal is pre-processed for spot presence survey over the maximum of 10x10 pixel field. This allows the third phase to begin: the tracking phase.

The centering phase has occasionally resulted in loss of the star from the field of view. Fig. 3.2-1 reports the percentage of the stars lost in centering for the period 3<sup>rd</sup> February 2003 to 26<sup>th</sup> October 2008. It can be seen that only four stars, mainly weak stars (higher star id means higher magnitude) are lost during the centering phase between 4% and 9 % of their planned observations. As the monitoring shows neither a trend nor excessively high percentages of loss, there is no need for the moment to reject any star from the catalogue, and there is no indication of instrument-related problems. Now with the instrument in a new operation scenario, the stars could be also lost due to the anomaly “elevation voice coil command saturation” even if the instrument is not going anymore to Stand by / Refuse mode (section 3.3).

### Statistics on stars lost in centering: 03-FEB-2003 until 26-OCT-2008

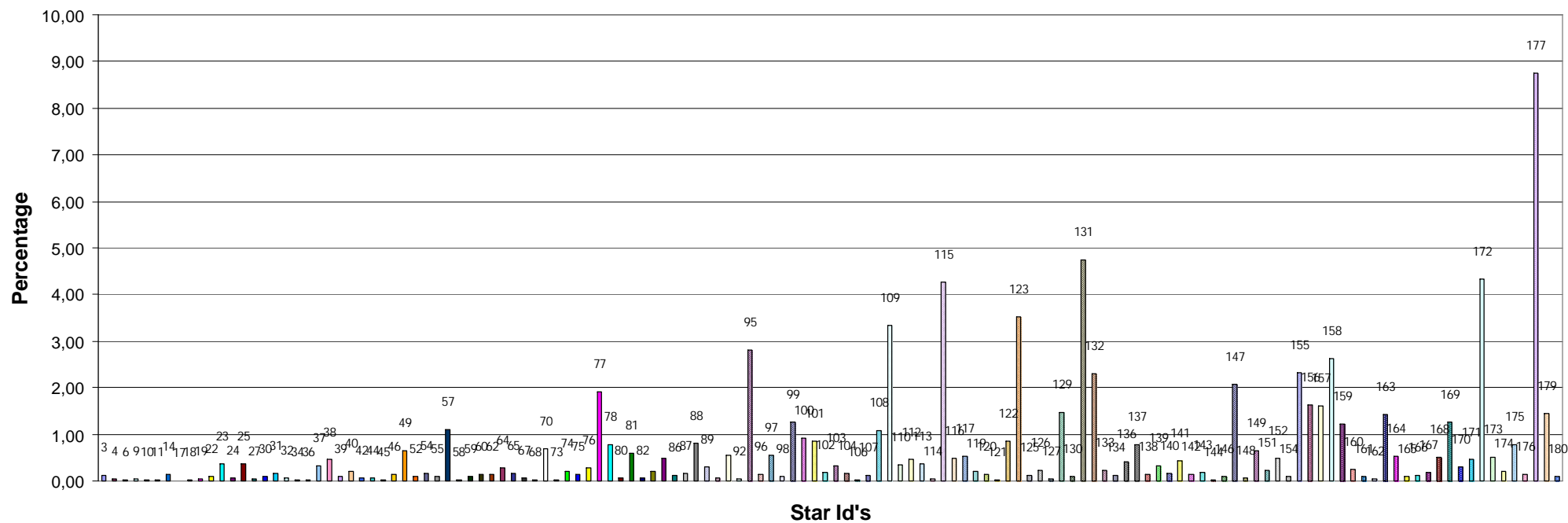


Figure 3.2-1: Statistics on stars that have been lost during the centering phase. The number above the columns corresponds to the Star ID

### 3.3 Stars lost due to VCCS anomaly

No VCCS anomaly during nominal operations.

### 3.4 Data Generation Gaps

The trend in percentage of available NRT data within the archives PDHS-K and PDHS-E is depicted in fig. 3.4-1 (when instrument was in operation). It is a good indicator on how the PDS chain is working in terms of generation and dissemination of data to the archives. The percentage is calculated once per week.

During the reporting period the availability of Level 0 and Level 1 NRT was higher than 99%.

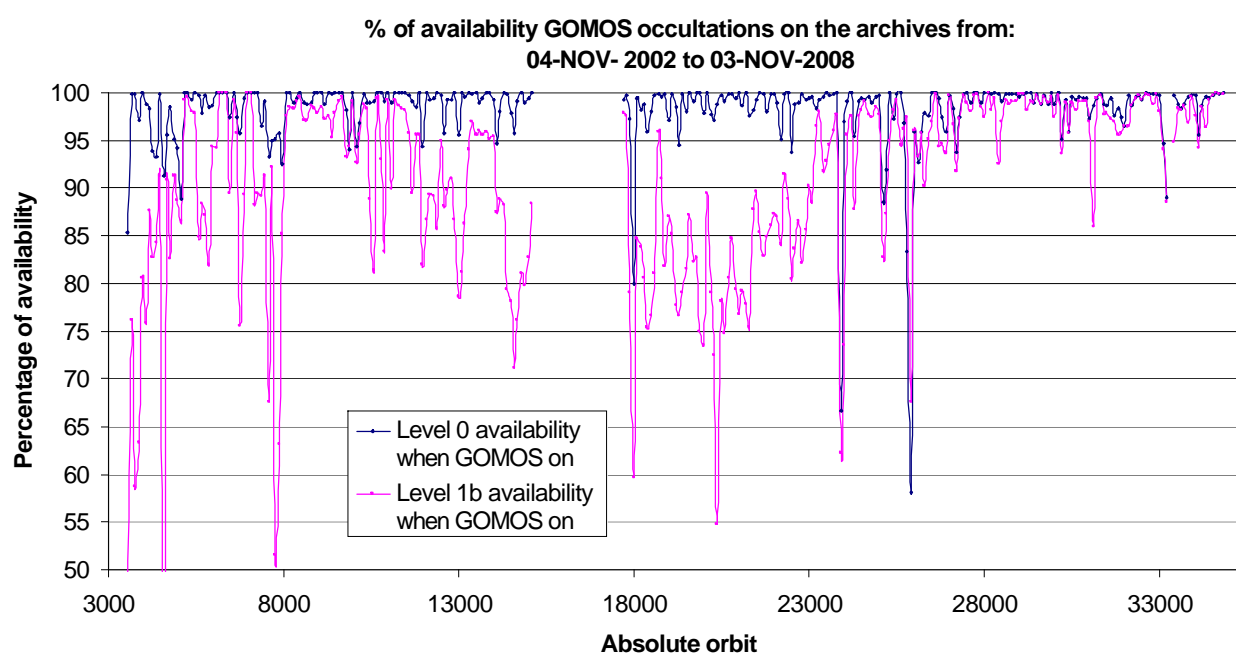


**Figure 3.4-1: Percentage of level 0 and level 1b data availability on the archives PDHS-E and PDHS-K**

Occultations planned to be acquired but for which no GOM\_NL\_\_0P data product has become available are presented in fig. 3.4-2 for the reporting period.

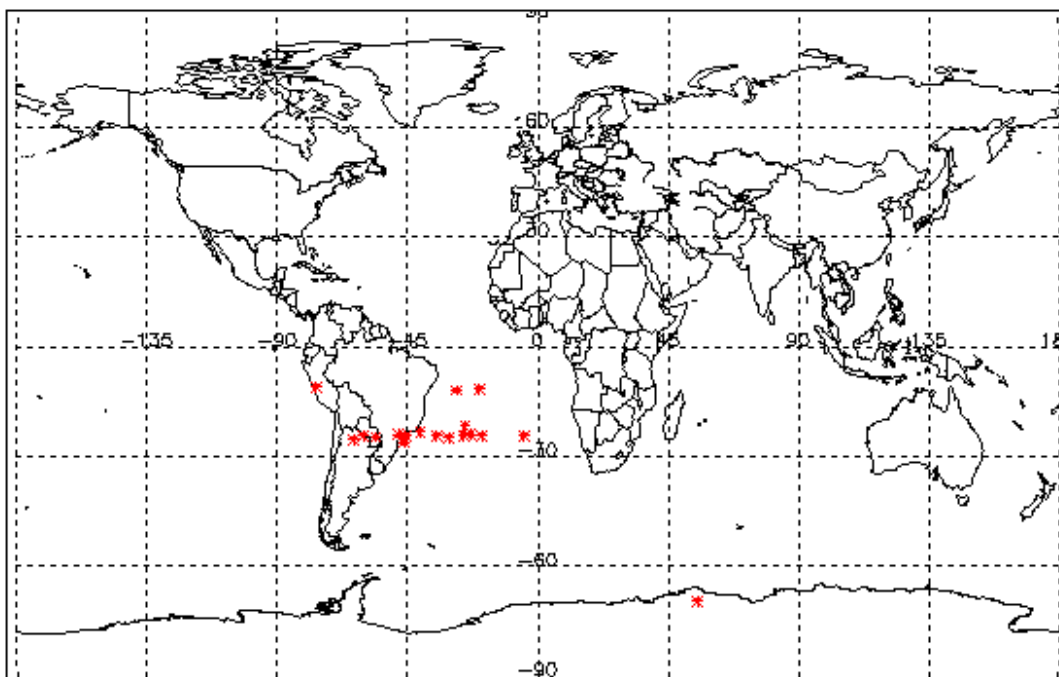


Figure 3.4-2: The red points are the occultation geo-location (starting) corresponding to planned data acquisitions for which no GOMOS level 0 product has become available

### 3.5 Data availability to users

Routine dissemination of higher-level products produced by the PDS to the users is enabled. Level 1b data are available on request to the EO Helpdesk ([EOHelp@esa.int](mailto:EOHelp@esa.int)), while level 2 data are available for the whole mission. For information on the passwords, please, contact the EO Helpdesk ([EOHelp@esa.int](mailto:EOHelp@esa.int)):

- Reprocessed products GOM\_NL\_\_2P are available at **the D-PAC ftp server** (name: **ftp-ops-dp.eo.esa.int**, IP-Address: **195.37.183.37**):  
<ftp://gomo2usr@ftp-ops-dp.eo.esa.int> from **August 2002 to 4<sup>th</sup> July 2006**.
- Near Real Time products GOM\_NL\_\_2P (generated three hours after sensing time) are available on the following servers:  
<ftp://gomosusr@oa-es.eo.esa.int> (ESRIN data). **A seven-day rolling archive has been set-up on this server.**  
<ftp://gomosusr@oa-ks.eo.esa.int> (KIRUNA data). **A seven-day rolling archive has been set-up on this server.**
- Consolidated products GOM\_NL\_\_2P (generated three weeks after sensing time) are available at D-PAC ftp server  
<ftp://gomo2usr@ftp-ops-dp.eo.esa.int> since **23 July 2006**

All data (reprocessed, NRT and consolidated) are processed with the same version of GOMOS processor.

## 4 INSTRUMENT CONFIGURATION AND PERFORMANCE

### 4.1 Instrument Operation and Configuration

#### 4.1.1 OPERATIONS SINCE BEGINNING OF MISSION

During the period end of March 2003 to July 2003 the azimuth range had to be decreased in steps (table 4.1-1) to avoid an instrument problem (“Voice\_coil\_command\_saturation” anomaly) that caused GOMOS to go into STAND BY/REFUSE mode. On July 2003 the driver assembly was switched to the redundant B-side and since that date the full azimuth range (-10.8, +90.8) was again available until the second major anomaly occurred on 25<sup>th</sup> January 2005. Between this date and until the instrument was declared operational again (29<sup>th</sup> August 2005), GOMOS has been operated for testing and anomaly investigation purposes in different operations scenarios. The changes in azimuth configuration during the whole mission until end of reporting period are summarized in table 4.1-1.

**Table 4-1: Historical changes in Azimuth configuration when GOMOS is in operations**

Date	Orbit	Minimum Azimuth (°)	Maximum Azimuth (°)	Comment
01-MAR-2002		-10.8	+90.8	Nominal
29-MAR-2003 17:40	5635	0.0	+90.8	Reduced
31-MAY-2003 06:22	6530	+4.0	+90.8	Reduced
16-JUN-2003 16:17	6765	+12.0	+90.8	Reduced
15-JUL-2003 01:39	7200	-10.8	+90.8	Nominal
25-JAN-2005 23:33	15200	tests	tests	Different configuration for testing purposes
29-AUG-2005 02:52	18280	-10	+10	Reduced
26-SEP-2005 01:32	18680	-5	+20	Reduced
03-OCT-2005 01:12	18780	-5	+15	Reduced
09-OCT-2005 21:30	18878	-5	+20	Reduced
12-MAR-2006 17:29	21080	+10	+35	Reduced
09-APR-2006 12:47	21480	+5	+30	Reduced
16-APR-2006 15:48	21580	0	+25	Reduced
30-APR-2006 15:08	21780	-5	+20	Reduced
07-MAY-2006 14:48	21880	0	+25	Reduced
14-MAY-2006 14:28	21980	+15	+40	Reduced
28-MAY-2006 13:47	22180	+20	+45	Reduced
04-JUN-2006 13:27	22280	+15	+40	Reduced
18-JUN-2006 12:47	22480	+20	+45	Reduced
25-JUN-2006 12:27	22580	0	+25	Reduced
02-JUL-2006 12:07	22680	-5	+20	Reduced
16-JUL-2006 11:27	22880	0	+25	Reduced
23-JUL-2006 11:07	22980	+10	+35	Reduced
06-AUG-2006 10:26	23180	0	+25	Reduced
27-AUG-2006 09:26	23480	+5	+30	Reduced
03-SEP-2006 09:06	23580	0	+25	Reduced
10-SEP-2006 08:46	23680	-5	+20	Reduced
01-OCT-2006 07:45	23980	+5	+30	Reduced
15-OCT-2006 07:05	24180	-5	+20	Reduced
22-OCT-2006 06:45	24280	0	+25	Reduced
29-OCT-2006 06:25	24380	-5	+20	Reduced
05-NOV-2006 06:05	24480	10	+35	Reduced
12-NOV-2006 05:45	24580	5	+30	Reduced
03-DEC-2006 04:44	24880	20	+45	Reduced
10-DEC-2006 04:24	24980	10	+35	Reduced

17-DEC-2006 20.50	25090	0	+25	Reduced
24-DEC-2006 03.44	25180	5	+30	Reduced
07-JAN-2007 03.04	25380	0	+25	Reduced
14-JAN-2007 02.44	25480	-5	+20	Reduced
21-JAN-2007 02.23	25580	0	+25	Reduced
28-JAN-2007 02.03	25680	-5	+20	Reduced
04-FEB-2007 01.43	25780	-10	+15	Reduced
11-FEB-2007 01.23	25880	-5	+20	Reduced
18-FEB-2007 01.03	25980	0	+25	Reduced
25-FEB-2007 00.43	26080	+5	+30	Reduced
04-MAR-2007 00.23	26180	+15	+40	Reduced
11-MAR-2007 00.03	26280	+20	+45	Reduced
24-MAR-2007 23.22	26480	0	+45	Reduced
31-MAR-2007 23.02	26580	+5	+30	Reduced
07-APR-2007 22.42	26680	+10	+35	Reduced
14-APR-2007 22.22	26780	+5	+30	Reduced
21-APR-2007 22.02	26880	0	+25	Reduced
28-APR-2007 21.42	26980	-5	+20	Reduced
12-MAY-2007 21.02	27180	20	+45	Reduced
19-MAY-2007 20.41	27280	+10	+35	Reduced
09-JUN-2007 19.41	27580	+15	+40	Reduced
16-JUN-2007 19.21	27680	-5	+20	Reduced
23-JUN-2007 19.01	27780	0	+25	Reduced
07-JUL-2007 18.21	27980	-5	+20	Reduced
04-AUG-2007 17:00	28380	0	+25	Reduced
11-AUG-2007 16.40	28480	5	+30	Reduced
18-AUG-2007 16.20	28580	0	+25	Reduced
26-AUG-2007 16.00	28680	10	+35	Reduced
04-SEP-2007 04.01	28816	+65	+90	Reduced: SATU-Y test
05-SEP-2007 06.51	28832	+10	+35	Reduced
08-SEP-2007 15.19	28880	+15	+40	Reduced
15-SEP-2007 14.59	28980	+20	+45	Reduced
22-SEP-2007 14.39	29080	-5	+15	Reduced
29-SEP-2007 14.19	29180	+5	+30	Reduced
13-OCT-2007 13.39	29378	10	+35	Reduced
20-OCT-2007 13.19	29480	0	+30	Reduced
24-OCT-2007 01.09	29530	0	+25	Reduced
27-OCT-2007 12.59	29580	10	+35	Reduced
10-NOV-2007 12.18	29780	-5	+20	Reduced
17-NOV-2007 11.58	29880	0	+25	Reduced
24-NOV-2007 11.38	29980	+5	+30	Reduced
01-DEC-2007 11.18	30080	+15	+40	Reduced
08-DEC-2007 10.58	30180	+10	+35	Reduced
11-DEC-2007 22.48	30230	+5	+35	Reduced
15-DEC-2007 10.38	30280	+5	+30	Reduced
22-DEC-2007 10.18	30380	0	+25	Reduced
05-JAN-2008 09.37	30580	-1	+24	Reduced
12-JAN-2008 09.17	30680	-2	+23	Reduced
19-JAN-2008 08.57	30780	-7	+18	Reduced
26-JAN-2008 08.37	30880	-2	+23	Reduced
02-FEB-2008 08.17	30980	-6	+24	Reduced
16-FEB-2008 07.37	31180	-8	+22	Reduced
23-FEB-2008 07.17	31280	-2	+28	Reduced
01-MAR-2008 06.56	31380	+5	+35	Reduced
08-MAR-2008 06:36	31480	+13	+43	Reduced
15-MAR-2008 06:16	31580	+10	+40	Reduced

22-MAR-2008 16:00	31686	+14	+44	Reduced
29-MAR-2008 05:36	31780	-1	+29	Reduced
05-APR-2008 05:16	31880	-8	+22	Reduced
12-APR-2008 04:56	31980	-4	+26	Reduced
19-APR-2008 04:36	32080	-10	+20	Reduced
03-MAY-2008 03:55	32280	-5	+25	Reduced
10-MAY-2008 03:35	32380	-6	+24	Reduced
17-MAY-2008 03:15	32480	+9	+39	Reduced
24-MAY-2008 02:55	32580	+14	+44	Reduced
31-MAY-2008 12:39	32686	+16	+46	Reduced
07-JUN-2008 02:15	32780	+18	+48	Reduced
14-JUN-2008 01:55	32880	+5	+35	Reduced
21-JUN-2008 01:35	32980	+6	+36	Reduced
28-JUN-2008 01:14	33080	-2	+28	Reduced
05-JUL-2008 00:54	33180	-10	+20	Reduced
19-JUL-2008 00:14	33380	0	+30	Reduced
25-JUL-2008 23:54	33480	+5	+35	Reduced
01-AUG-2008 23:34	33580	-1	+29	Reduced
08-AUG-2008 23:14	33680	-3	+27	Reduced
15-AUG-2008 22:54	33780	+12	+42	Reduced
23-AUG-2008 08:37	33886	+5	+35	Reduced
29-AUG-2008 22:13	33980	+4	+34	Reduced
05-SEP-2008 21:53	34080	+6	+36	Reduced
12-SEP-2008 21:33	34180	+15	+45	Reduced
27-SEP-2008 06:56	34386	+4	+34	Reduced
03-OCT-2008 20:33	34480	+7	+37	Reduced
10-OCT-2008 20:13	34580	+4	+34	Reduced
17-OCT-2008 19:53	34680	+2	+32	Reduced
01-NOV-2008 05:16	34886	+3	+33	Reduced

#### 4.1.2 CURRENT OPERATIONS AND CONFIGURATION

The planned GOMOS operations for the reporting period are identified in table 4.1-2. The operation scenario of GOMOS since 29<sup>th</sup> August 2005 until end of reporting month consists of:

- Planning 2 orbits per sequence (nominal were 5): this is done because in case of a voice coil failure with subsequent loss of star observation, the maximum loss of consecutive observations cannot exceed two orbits.
- Reduced azimuth field of view (nominal was  $[-10^{\circ}, +90^{\circ}]$ ): as the anomaly occurs during the rallying of the telescope in the preparation for the star observation, it has been decided to reduce the field of view in order to minimize the failure occurrence probability. Different ranges have been used during the reporting period (table 4.1-1) in order to optimize the number of occultations per orbit.

Since 2<sup>nd</sup> February 2008 the azimuth window was moved from 25 to 30 degrees.

Following the ARB held on the 21<sup>st</sup> August to discuss the VCCS anomalies it was agreed to set the minimum threshold of the GOMOS azimuth measurement window at  $+2^{\circ}$ . The reason being that with an aimed ENVISAT mission up to 2014, the GOMOS mechanics should be operated with care, in particular VCCS may translate into mechanism fatigue, and thus the consensus among the teleconference participants is to avoid any VCCS at all.

**Table 4-2: GOMOS planned operations. The planning is built on a 2-orbit sequence basis (2 orbits with the same stars)**

UTC Start	Start Orbit	Stop Orbit	Mode (Asynchronous or Synchronous)	Calibration (CAL) Dark Sky Area (DSA) or Nominal (Nom)
27-SEP-2008 13.39.22	34390	34477	S	Nom
03-OCT-2008 17.12.04	34478	34478	A	Nom
03-OCT-2008 20.33.16	34480	34577	S	Nom
10-OCT-2008 16.51.57	34578	34578	A	Nom
10-OCT-2008 20.13.08	34580	34677	S	Nom
17-OCT-2008 16.31.49	34678	34678	A	Nom
17-OCT-2008 19.53.01	34680	34777	S	Nom
24-OCT-2008 16.11.42	34778	34778	A	Nom
24-OCT-2008 19.32.54	34780	34877	S	Nom
31-OCT-2008 15.51.35	34878	34878	A	Nom
31-OCT-2008 19.12.47	34880	34885	A	CAL
01-NOV-2008 05.16.22	34886	34887	A	CAL
01-NOV-2008 08.37.34	34888	34889	A	CAL

There was no new Configurable Table Interface (CTI) uploaded to the instrument. The files used since the beginning of the mission are in table 4.1-3. The yellow ones are the current ones in use.

**Table 4-3: Historic CTI Tables**

CTI filename		Dissemination to FOCC
SMP	CTI_SMP_GMVIEC20030716_123904_00000000_00000004_20030715_000000_20781231_235959.N1	16-JUL-2003
	CTI_SMP_GMVIEC20021104_075734_00000000_00000003_20021002_000000_20781231_235959.N1	06-NOV-2002
	CTI_SMP_GMVIEC20021002_082339_00000000_00000002_20021002_000000_20781231_235959.N1	07-OCT-2002
	CTI_SMP_GMVIEC20020207_154455_00000000_00000000_20020301_032709_20781231_235959.N1	21-FEB-2002
STP	CTI_STP_GMTIEC20021104_080137_00000000_00000000_20021002_000000_20781231_235959.N1	04-NOV-2002
	CTI_STP_GMVIEC20021002_083222_00000000_00000000_20021002_000000_20781231_235959.N1	02-OCT-2002

## 4.2 Limb, Illumination conditions and instrument gain setting

The **limb** and the **illumination condition** are two parameters that can confuse the user community. In table 4.2-1 there are specified the product parameter (level 1b and level 2 of processor GOMOS/4.02 operational until 8<sup>th</sup> August 2006) where the flag is located, the meaning and the source. The difference between the limb (SPH/bright\_limb) and the illumination condition (SUMMARY\_QUALITY/limb\_flag) is that the first one is coming from the mission scenario and the second is coming from the processing (defined from the computation of the sun zenith and azimuth angles at both instrument and tangent point locations). The SPH/bright\_limb is for some occultations set to “dark” in the mission scenario while they are in fact in bright limb illumination conditions. To select the highest quality data for scientific applications, data with SUMMARY\_QUALITY/limb\_flag equal to ‘0’ should be used (see also the disclaimer: <http://envisat.esa.int/dataproducts/availability/disclaimers>). The instrument gain settings are also specified in table 4.2-1 (they depend on the mission scenario flags) just for completeness of information. The same is valid for the prototype version GOPR\_6.0a\_6.0a and following ones (including the one that was used for the second reprocessing of 2002-2005 years), where the **limb** is in fields SPH/bright\_limb and SUMMARY\_QUALITY/dark\_bright\_limb and the **illumination condition** is in field SUMMARY\_QUALITY/obs\_ill\_cond. For these prototypes **and the**



processor GOMOS/5.00 in operations since 8<sup>th</sup> August 2006, the illumination condition can have five values (see table 4.2-2).

**Table 4-4: Relationship between limb, illumination condition flags and instrument gain settings (IPF version GOMOS/4.02 and previous)**

Products parameter	SPH/bright_limb	0 = Dark	1 = Bright	Coming from mission scenario
	SUMMARY_QUALITY/limb_flag	0 = Full Dark 1 = Bright 2 = Twilight	1 = Bright 2 = Twilight	In the geolocation process the sun zenith angle is computed and the occultation then is flagged accordingly
Instrument Gain	SPA Gain	3 (2)	0	Gain setting for spectrometer A. In parenthesis, values valid only for Sirius occultations (starID=1)
	SPB Gain	0	0	Gain setting for spectrometer B

**Table 4-5: Relationship between limb, illumination condition flags and instrument gain settings (IPF version GOMOS/5.00 and following ones; prototype version GOPR 6.0a\_6.0a and following ones)**

Products parameter	SPH/bright_limb SUMMARY_QUALITY/dark_bright_limb	0 = Dark	1 = Bright	Coming from mission scenario
	SUMMARY_QUALITY/obs_ill_cond	0 = Full Dark 1 = Bright 2 = Twilight 3 = Straylight 4 = Twi.+Stray		In the geolocation process the sun zenith angle is computed and the occultation is then flagged accordingly
Instrument Gain	SPA Gain	3 (2)	0	Gain setting for spectrometer A. In parenthesis, values valid only for Sirius occultations (starID=1)
	SPB Gain	0	0	Gain setting for spectrometer B

### 4.3 Thermal Performance

Since the beginning of the mission, the hot pixel and RTS phenomena have been producing a continuous increase of the dark charge signal within the CCD detectors (see section 4.5.1). In order to minimize this effect, three successive CCD cool downs were performed in orbits 800 (25<sup>th</sup> April 2002), 1050 (13<sup>th</sup> May 2002) and 2780 (11<sup>th</sup> September 2002) with a total decrease in temperature of 14 degrees.

Fig. 4.3-1 and 4.3-2 display, respectively, the overall temperature variation and the temperature variation around the Ascending Node Crossing (ANX) time with a resolution of 0.4 degrees (coding accuracy for level 0 data).

The CCD temperatures show the expected global increase due to the radiator ageing. Another expected variation of the temperatures, the seasonal one, can be also observed: at the beginning of mission the amplitude was around 0.8 but now it is around 1.5 degrees. The peaks that occur mainly in spectrometer B1 and B2 are also to be noted. They happen a little before the ANX for some consecutive orbits and every 8-10 days. Their origin is not known, as we did not find any correlation between these peaks and other activities carried out by other ENVISAT instruments.

The CCD temperature at almost the same latitude location (fig. 4.3-2) is monitored in order to detect any inter-orbital temperature variation. The abnormal decreases observed sometimes in all detectors are after GOMOS switch off periods, when the instrument did not have enough time to reach the nominal temperature before starting the measurements.

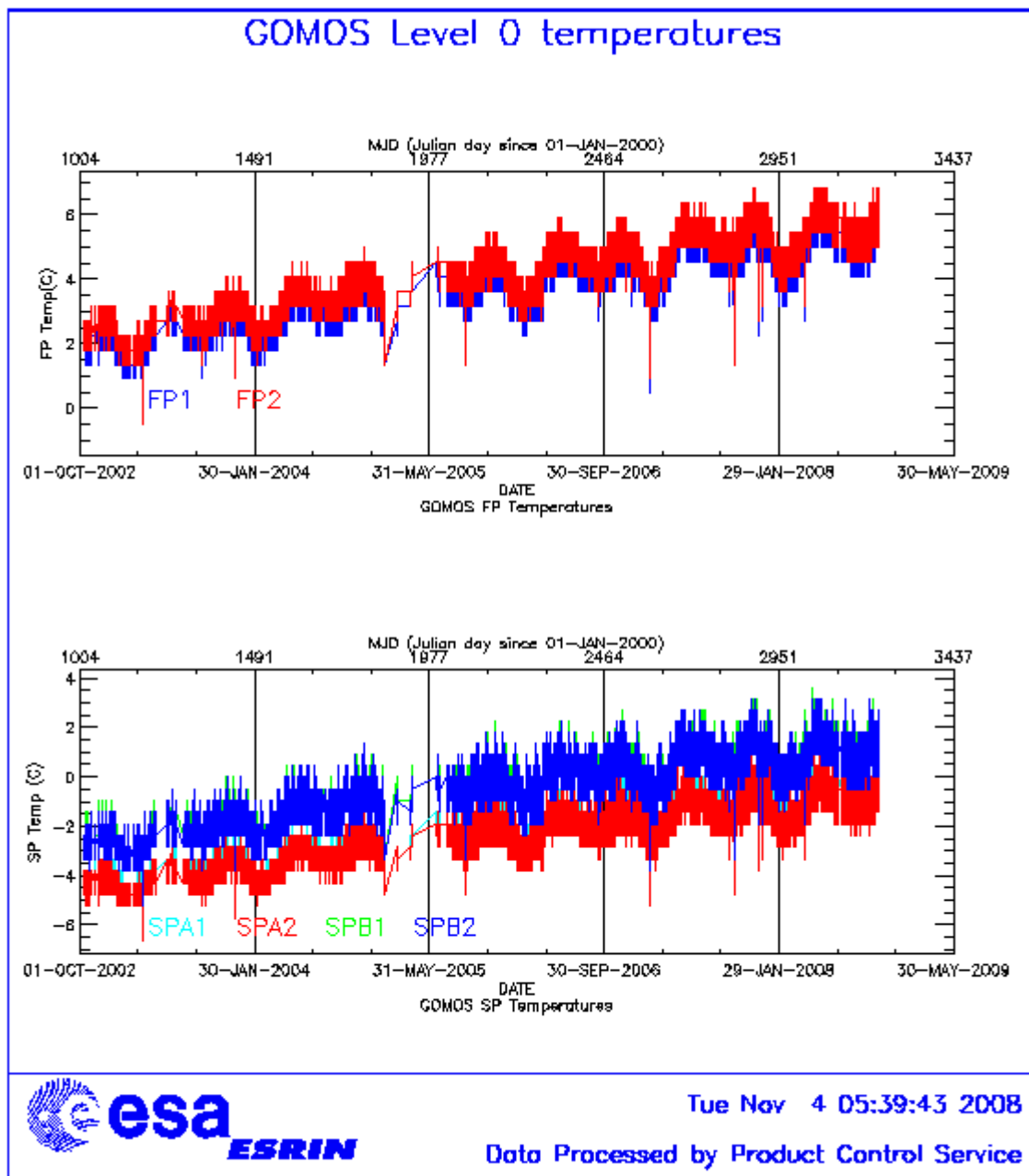


Figure 4.3-1: Level 0 temperature evolution of all GOMOS CCD detectors since October 2002 until the end of the reporting period

During the reporting period, the orbital temperature variation of the detector SPB2 for ascending and descending passes (fig. 4.3-3 and 4.3-4) is nominal (around 3 degrees). The stability of the temperature during the orbit is important because it affects the position of the interference patterns. The phenomenon of the interference is present mainly in SPB and this Pixel Response Non-Uniformity (PRNU) is corrected during the processing.



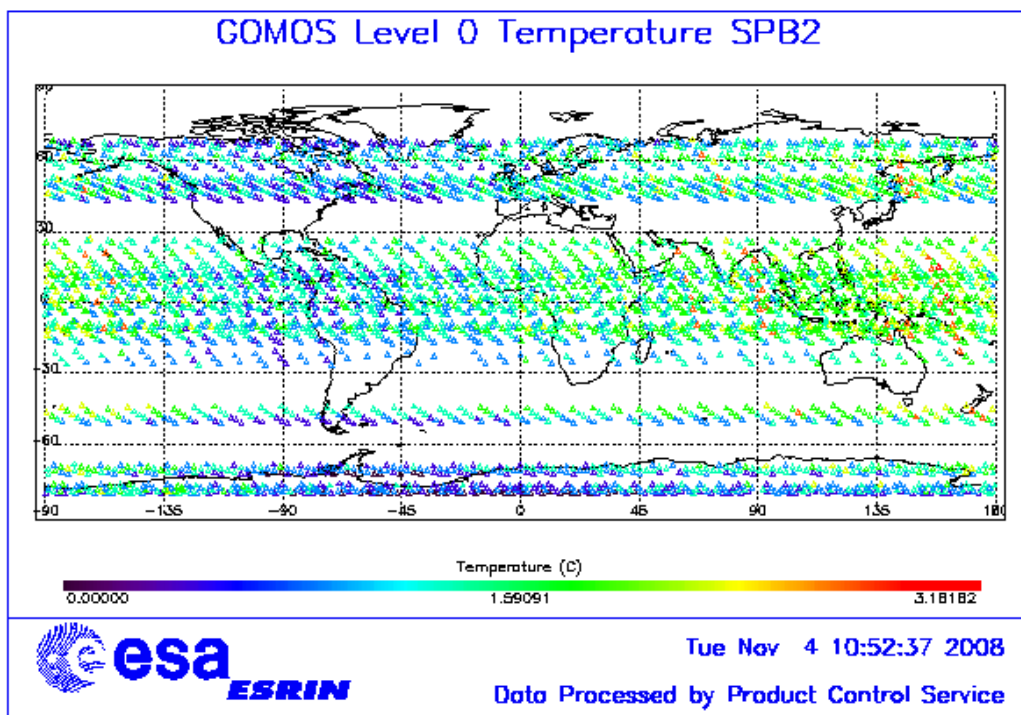


Figure 4.3-3: Ascending orbital variation of SPB2 temperature during reporting period

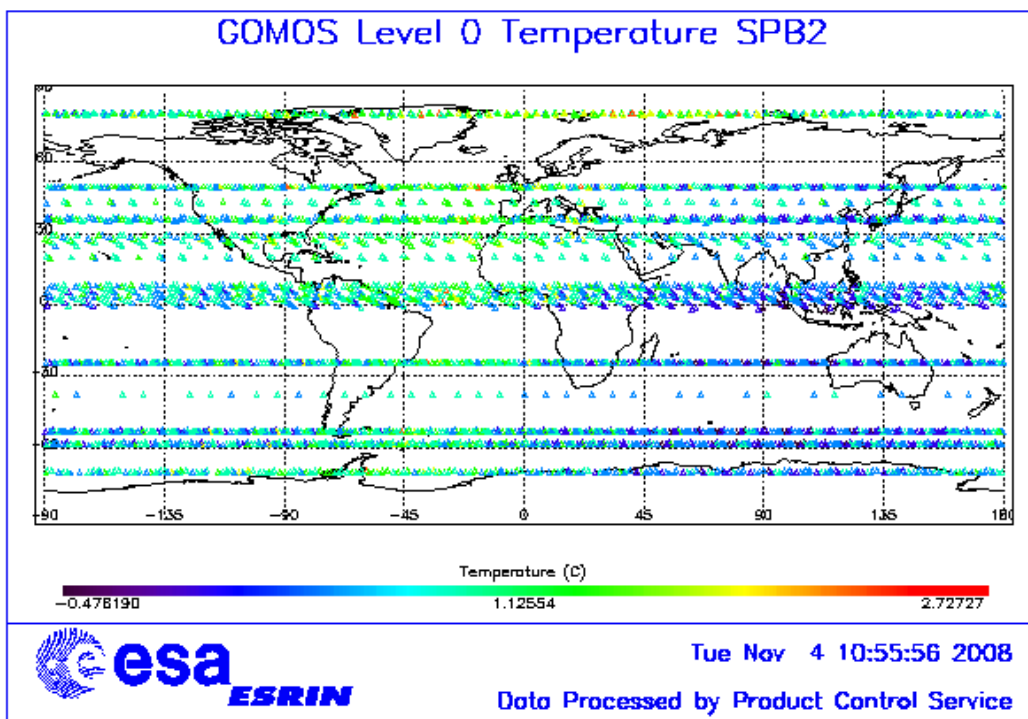


Figure 4.3-4: Descending orbital variation of SPB2 temperature during reporting period

### 4.4 Optomechanical Performance

- Version GOMOS/4.00 and previous ones: in the GOMOS processor versions GOMOS/4.00 and previous, the spectra are expected to be aligned along CCD lines, and therefore use only a single average line index per CCD. In table 4.4-1, the mean values of the location of the star signal for all the calibration analysis done is reported. The ‘left’ and ‘right’ values are calculated (the whole interval is not used) because the spectra present a slight slope, more pronounced in spectrometer B. In table 4.4-2, mean values of the location of the star signal are calculated for some specific wavelength intervals. These intervals have been changed between the calibration performed in September 2002 and the ones performed afterwards (until November 2003). Table 4.4-3 reports the average location of the star spot on the photometer 1 and 2 CCD.
- Version GOMOS/4.02: in this processor version operational since 23<sup>rd</sup> March 2004 until 8<sup>th</sup> August 2006, a Look Up Table (LUT) gives the line index of the spectra location as a function of the wavelength. The values obtained during calibration exercises are shown in table 4.4-4. These values should be similar to the ones of the LUT; otherwise the LUT should be updated. However this characterization curve is not exactly the location of the star spectrum on the CCD but rather a combination of this position and some artefact created by the shape of the instrument optical point spread function (PSF). The exact shape is actually a straight line (especially for SPB) that has been characterised in 2005.
- Current version GOMOS/5.00 (since 8<sup>th</sup> August 2006): the exact shape of the CCD spectra location curve (which is a straight line) that has been characterised in 2005 was implemented in the current set of GOMOS ADFs. The position of the spectra convoluted with the PSF is calculated during the processing.

**Table 4-6: Mean value of the location of the star signal during the occultation at the edges of every band (mean over 50 values, filtering the outliers)**

	UV (SPA1) left/right	VIS (SPA2) left/right (Inverted spectra)	IR1 (SPB1) left/right	IR2 (SPB2) left/right
11/09/2002	80.7/80.7	79.8/79.5	82.8/81.9	83.1/82.1
01/01/2003	80.7/80.6	79.8/79.5	82.8/82.0	83.2/82.2
17/07/2003 & 02/08/2003	80.7/80.7	79.8/79.5	82.8/81.9	83.1/82.1
08/11/2003	80.7/80.6	79.8/79.5	82.8/81.9	83.1/82.1

**Table 4-7: Mean value of the location of the star signal during the occultation (as table 4.4-1) but now within some wavelength intervals**

	UV (SPA1)	VIS (SPA2)	IR1 (SPB1)	IR2 (SPB2)
11/09/2002 wl range (nm)	80.8 [300-330]	79.8 [500-530]	82.6 [760-765]	82.9 [937-942]
01/01/2003 wl range (nm)	80.6 [350-360]	78.6 [650-670]	81.6 [760-765]	80.3 [935-945]
02/08/2003	80.6	79.7	82.5	82.8
08/11/2003	80.6	79.9	82.4	82.8

**Table 4-8: Average column and row pixel location of the star spot on the photometer CCD during the occultation**

	FP1 (column/row)	FP2 (column/row)
11/09/2002	11/4	5/5
01/01/2003	10/4	6/4.9
02/08/2003	10/4	6/5
08/11/2003	10/4	6/5

**Table 4-9: Location of the star signal on the CCD's**

Pixel Column	LUT (Pixel line)	Calibration on 10-APR-2004	Calibration on 04-DEC-2004	Calibration on 27-NOV-2005	Calibration on 19-FEB-2006	Calibration on 14-MAY-2006 and 11-JUN-2006
0	80.59	80.80	80.67	80.93	80.67	80.85
20	80.46	80.60	80.44	80.32	80.43	80.49
449	80.42	80.50	80.42	80.40	80.53	80.56
450	79.25	79.39	79.30	79.16	79.30	79.35
900	79.50	79.63	79.57	79.36	79.45	79.61
1415	79.70	79.76	79.76	80.00	79.81	79.93
1416	82.64	82.80	82.88	82.95	82.76	82.81
1500	82.31	82.60	82.66	82.63	82.58	82.55
1600	82.12	82.22	82.30	82.35	82.41	82.20
1700	81.97	82.04	82.08	82.09	82.05	82.06
1750	81.89	81.98	82.03	82.00	81.92	81.97
1800	81.78	81.91	81.96	81.93	81.83	81.98
1835	81.68	81.88	81.94	81.96	81.79	81.91
1836	82.98	83.10	83.10	83.27	83.17	83.08
2000	82.78	82.90	82.94	83.04	82.83	82.93
2100	82.33	82.70	82.73	82.82	82.83	82.67
2150	82.17	82.40	82.54	82.79	82.70	82.49
2350	81.83	82.00	82.00	82.68	81.96	82.11

## 4.5 *Electronic Performance*

### 4.5.1 DARK CHARGE EVOLUTION AND TREND

The trend of Dark Charge (DC) is of crucial importance for the final quality of the products, and is therefore subject to intense monitoring. As part of the DC there is:

- “Hot pixels”, a pixel is “hot” when its dark charge exceeds its value measured on ground, at the same temperature, by a significant amount.
- RTS phenomenon (Random Telegraphic Signal), it is an abrupt change (positive or negative) of the CCD pixel signal, random in time, affecting only the DC part of the signal and not the photon generated signal.

The temperature dependence of the DC would make this parameter a good indicator of the DC behaviour, but the hot pixels and the RTS are producing a continuous increase of the DC (see trend in fig. 4.5-1 and 4.5-2). To take into account these phenomena, since version GOMOS/4.00 (the current one is GOMOS/5.00) a DC map per orbit is extracted from a Dark Sky Area (DSA) observation performed around ANX (full dark conditions). For every level 1b product (occultation), the actual thermistor temperature of the CCD is used to convert the DC map measured around ANX into an estimate of the DC at the time (and different temperature) of the actual occultation. When the DSA

observation is not available, the DC map inside the calibration product that was measured at a given thermistor reference temperature is used; again, the actual thermistor temperature of the CCD is used to compute the actual map. Table 4.5-1 reports the list of products that used the DC maps inside the calibration file due to the non-availability of DSA observation. A “CAL DC map with no T dep.” means that, as the temperature information was not available for that occultation, the DC map used is exactly the one inside the Calibration product.

The “quality ranking” of the products depending on DC correction performed is as follows:

- Best quality: products with DC correction using DSA observation inside the orbit
- Less quality than previous ones: products with DC correction using the map inside the calibration product, thermal corrected (‘DC map used’ in table 4.5-1)
- Less quality than previous ones: products with DC correction using the map inside the calibration product, no thermal corrected (‘DC map with no T dep.’ in table 4.5-1)

**Table 4-10: Table of level 1b products that used the Calibration DC maps instead of the DSA observation. During the reporting month, all products analyzed used the DSA for the DC computation**

Product name	DC information
-	-

The average DC inserted by the processor into the level 1b data products for the spectrometers SPA1 and SPB2 (per band: upper, central and lower) is plotted in fig. 4.5-1 and 4.5-2. The abnormal decreases observed sometimes in all detectors are due to the temperature decreases that occur after GOMOS switch off periods. The same DC values are plotted in fig. 4.5-3 but for some occultations belonging only to the reporting month.

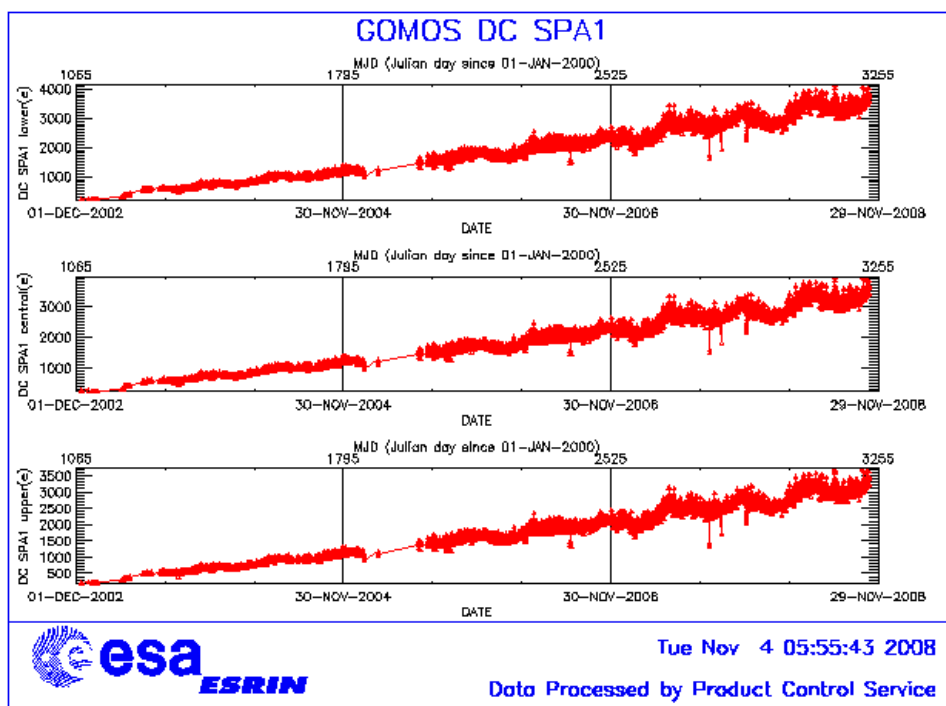


**Figure 4.5-1: Mean DC evolution on SPA1 since 15<sup>th</sup> December 2002 until the end of the reporting period**

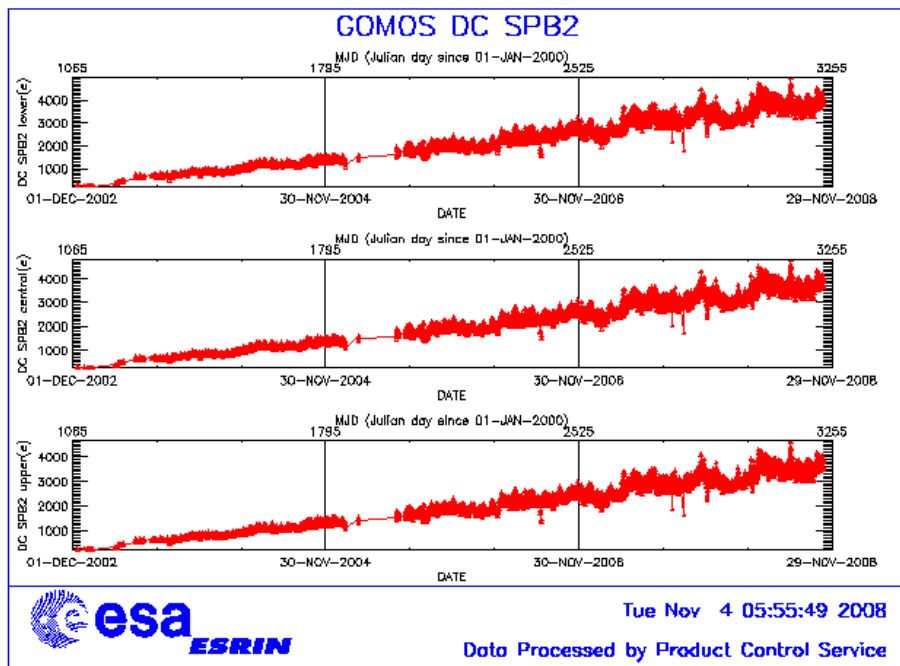


Figure 4.5-2: Mean DC evolution on SPB2 from 15<sup>th</sup> December 2002 until the end of the reporting period

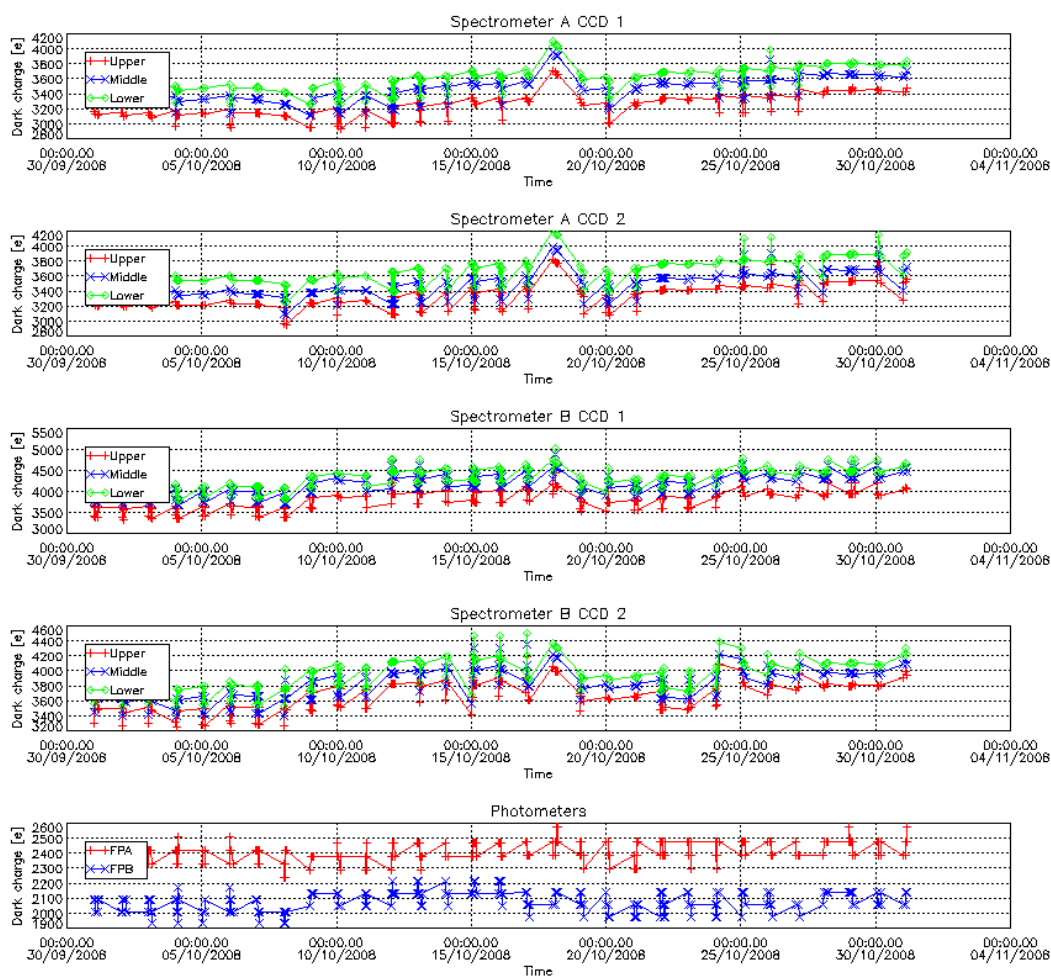


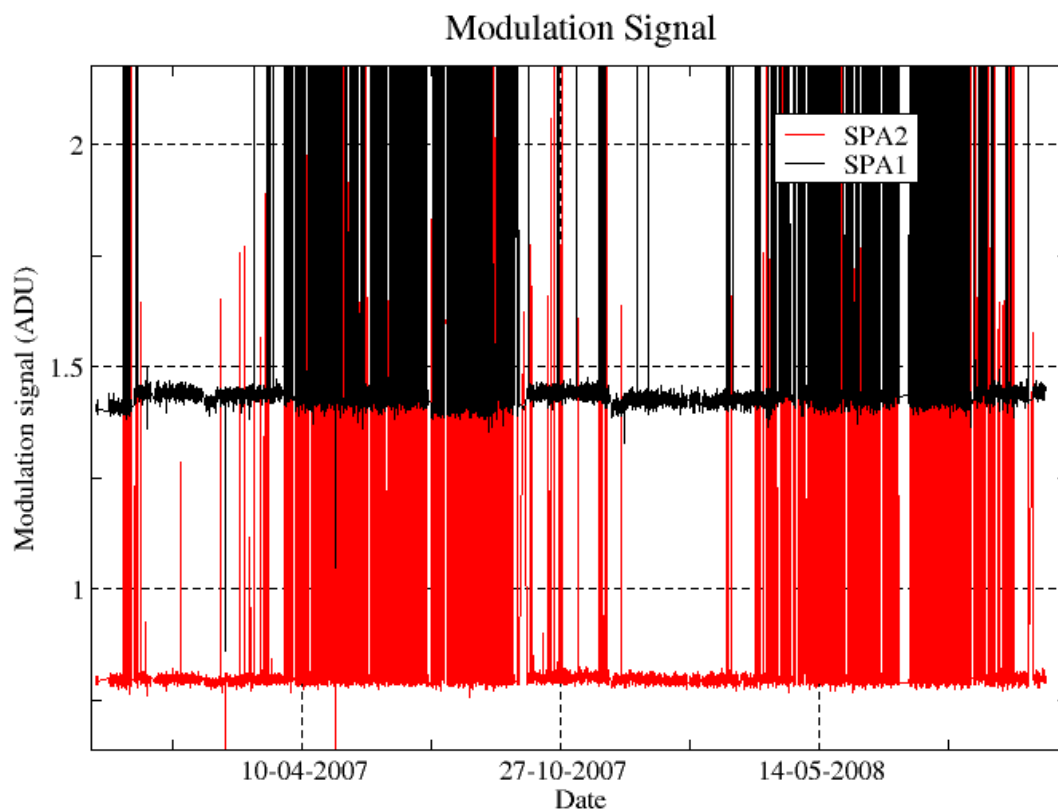
Figure 4.5-3: Mean Dark Charge of spectrometers during the reporting period



## 4.5.2 SIGNAL MODULATION

A parasitic signal was found to be systematically present, added to the useful signal, for the spectrometers A and B (fig. 4.5-4). The modulation is corrected in the data processing for spectrometers A1 and A2, for spectrometer B it has much smaller amplitude and so it is not corrected.

The values of the modulation (fig. 4.5-4) are daily extracted and plotted; they should not be very different from the ones coded into the processor: 1.40 ADU for SPA1 and 0.76 ADU for SPA2.



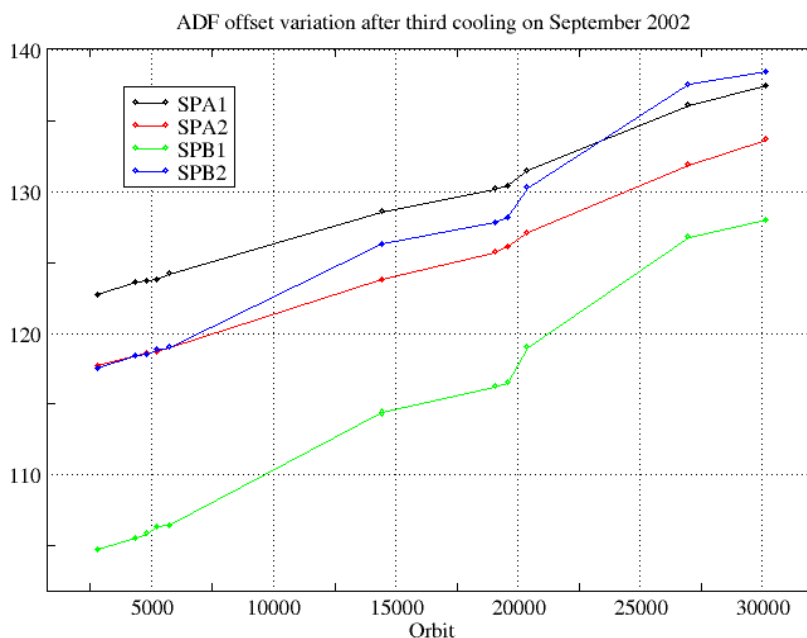
**Figure 4.5-4: Modulation signal**

Fig. 4.5-4 shows high values during summer time for the ESRIN data, it now being confirmed that the South Atlantic Anomaly is the cause of these unexpected peaks. The quality of ESRIN data, in particular over the SAA zone, is impacted but the measure of this impact is under investigation. However, in the second half of the months of October for all years (2004-2007) the peaks are smaller because the DSA zone where the data are taken for this analysis is moving towards the Northern Hemisphere. At the end of October the DSA zone is definitely chosen by the planning system in the Northern Hemisphere (to fill the criteria 'DSA in full dark limb conditions') and the high peaks disappear.

## 4.5.3 ELECTRONIC CHAIN GAIN AND OFFSET

No new electronic chain gain and offset calibration has been done during the reporting period. The routine monitoring of the ADC offset is a good indicator of the ageing of the instrument electronics. The fig. 4.5-5 presents the evolution of the calibrated ADC offset for each spectrometer electronic chain. The unexpected increase of this offset seems to be due to an external contribution. In the ADC offset calibration procedure, linearity observations are used with two integration times of 0.25 and 0.50

seconds to extrapolate to an integration time of 0 seconds that gives the complete chain offset and not only the ADC offset. The complete offset contains any possible offsets, and especially the static dark charge (i.e. the dark charge that does not depend on the spectrometer integration time). The presence of vertical lines visible in the measurement maps in spatial spread monitoring mode confirms that the memory area of the CCD is affected by the generation of hot pixels. These new hot pixels are one contributor to the increase observed in fig. 4.5-5.



**Figure 4.5-5: ADC offset evolution for each spectrometer electronic chain**

A current QWG task consists in completing the analysis to confirm that the offset increase is also due to the expected dark charge increase in the memory area due to ageing. This can be proven by the study of the noise due to the increased dark charge. The increase of ADC offset will be assumed to be equal to the increase of ‘static dark charge’ and the corresponding noise will be computed and compared to the increase of the residual of the signal variance.

If we keep the ADC offset constant, as it is also used to compute the dark charge at band level (which is used to correct the samples in the level 1b processing), the increase of the static dark charge - not taken into account in the ADC offset - is compensated by an artificial increase of the calibrated dark charge. So, the star and limb spectra are correctly corrected for dark charge. A small bias can be added to the instrument noise due to the incorrect dark charge level. Anyway, this quantity is not large enough to require a modification of the ADC offset value.

## 4.6 Acquisition, Detection and Pointing Performance

### 4.6.1 SATU NOISE EQUIVALENT ANGLE

The Star Acquisition and Tracking Unit (SATU) noise equivalent angle (SATU NEA) consists of the statistical angular variation of the SATU data above the atmosphere. The mean of the standard deviation (STD over the 50 values per measurement) above 105 km are computed for every occultation, giving two values per occultation: one in the ‘X’ direction, one in the ‘Y’ direction. A mean value per day in

every direction and limb is calculated and monitored in order to assess instrument performance in terms of star pointing (fig. 4.6-1). Also monthly averages are calculated and plotted (fig. 4.6-2). The thresholds are 2 and 3 micro radians in ‘X’ and ‘Y’ directions respectively. Before May 2003, data above 90 km have been considered (instead of 105 km) but from May 2003 on, data taken in the mesospheric oxygen layer (located around 100 km altitude) have been avoided because they could cause fluctuations on the SATU data. Also the products with errors (error flag set) are discarded from May 2003 onwards.

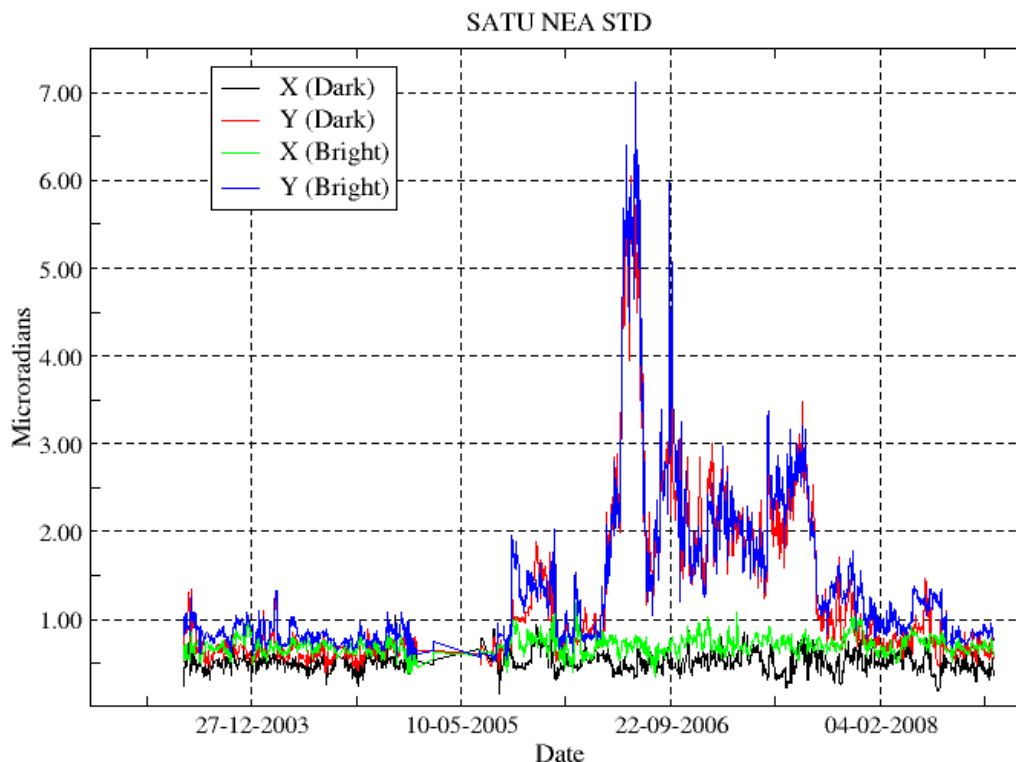


Figure 4.6-1: Average value per day of SATU NEA STD above 105 km

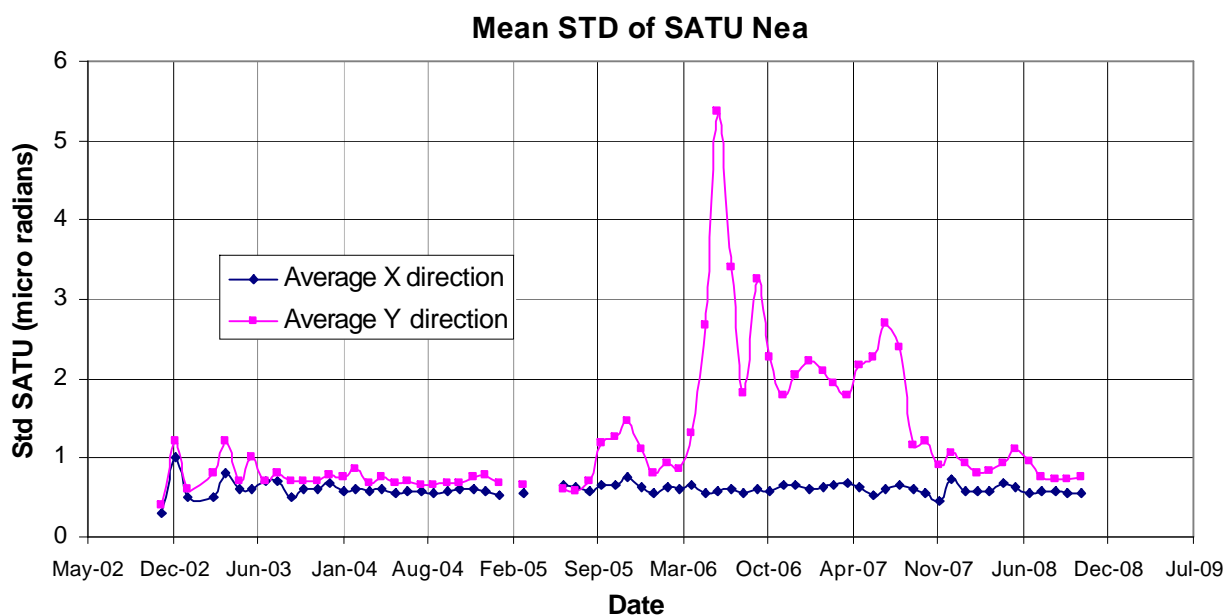


Figure 4.6-2: Average value per month of SATU NEA STD above 105 km

As can be seen in fig. 4-6.1, the SATU NEA had a sudden increase on 8<sup>th</sup> September 2005 mainly in ‘Y’ axis. These values remained high, fluctuating between 1 and 1.8 microrad until December 2005 when they came back to the values they used to be before the increase of September. The reason why there was higher noise in the data causing the jump in daily SATU average is not known.

A different problem was present since mid April 2006 until October 2007. A gradual increase of the daily SATU ‘Y’ mean was observed. This increase was due to fluctuations of the SATU ‘Y’ data observed at the beginning of nominal occultations (starting at 130 km that corresponds to an elevation angle of around 65°). The decrease of the start elevation angle of the occultation has no impact on the amplitude of the SATU ‘Y’ fluctuations. Investigations carried out by the ESL, ESA and industry pointed to a problem on the SFM (mechanical or electrical) and not to a problem on the SATU itself. Since October 2007 the fluctuations have disappeared and as a consequence the daily SATU ‘Y’ average has come back below the threshold set to 3 micro radians.

The results for some occultations belonging to previous months (monthly averages) are presented in fig. 4.6-2, where the change in trend in September 2005 and May 2006, mainly for the ‘Y’ axis is visible.

## 4.6.2 TRACKING LOSS INFORMATION

This verification consists of the monitoring of the tangent altitude at which the star is lost. It is an indicator of the pointing performance although it is to be considered that star tracking is also lost due to the presence of clouds and hence not only due to deficiencies in the pointing performance. Therefore, only the detection of any systematic long-term trend is the main purpose of this monitoring. The recent results are presented in fig. 4.6-3 and 4.6-4:

- The dependence of the altitude at which tracking is lost on the magnitude of the star is very small because the tracking is mainly lost due to the refraction and the scintillation that depend on the atmospheric conditions.
- The azimuth of some stars could be very near to the reduced instrument azimuth edges and therefore there could be occultations planned to have a duration very small (2, 6, 10...seconds). To avoid planning this kind of useless occultation, it has been decided to set the minimum occultation duration value to 25 seconds. Fig. 4.6-3 shows one star lost at an altitude higher than 30 km which corresponds either with an occultation with duration around 25-30 seconds or with a partial occultation (the entire occultation is included within the following orbit data file).
- In bright limb it is not expected that the stars are lost at very low altitudes due to the amount of light arriving to the pointing system mainly when the refraction effects start to be important. We see from fig. 4.6-4 that there are some stars lost at altitudes around 4 km. This occurs when the pointing system is not able to point to the star anymore but, instead of finishing the occultation, it continues to track light until the planned duration is reached.
- Daily statistics are given in fig. 4.6-5 (calculated using 50 products per day). The high peaks in standard deviation before 25<sup>th</sup> January 2005 are due to the long lasting occultations or partial occultations (the entire occultation is included within the following orbit data). The ones during June/July/August 2005 are due to the tests performed for the anomaly investigation. After 29<sup>th</sup> August 2006 the peaks are due to the “short occultations” or partial occultations.
- Monthly statistics are given in fig. 4.6-6 (calculated using 50 products per day) where the change in trends, mainly for dark limb, is visible for the period of GOMOS testing.

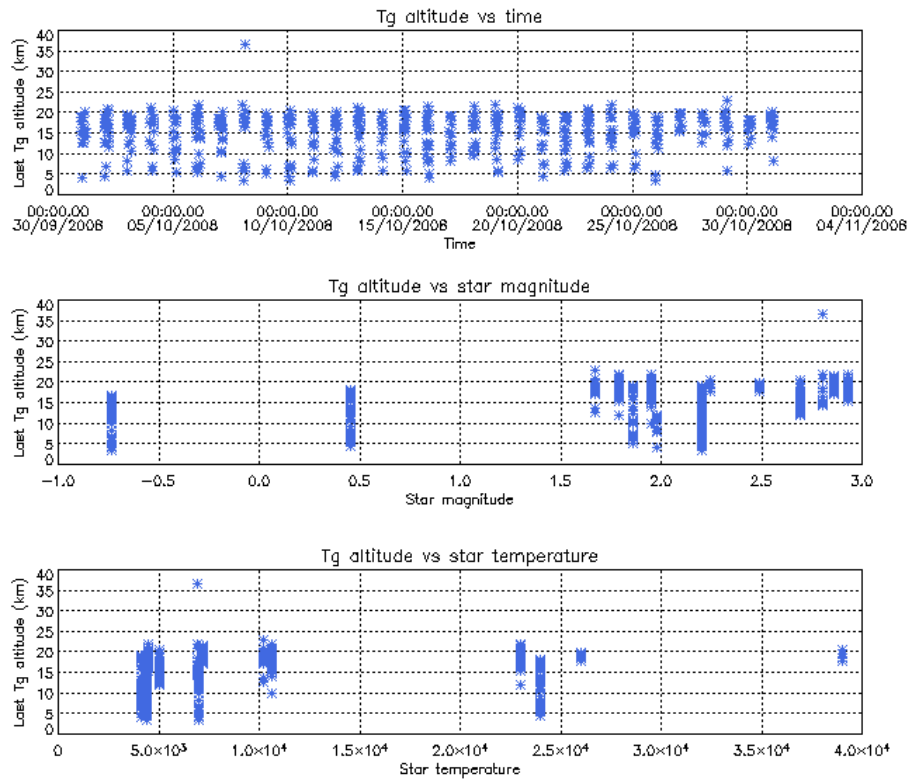


**Figure 4.6-3: Last tangent altitude of the occultation (dark limb), point at which the star is lost**

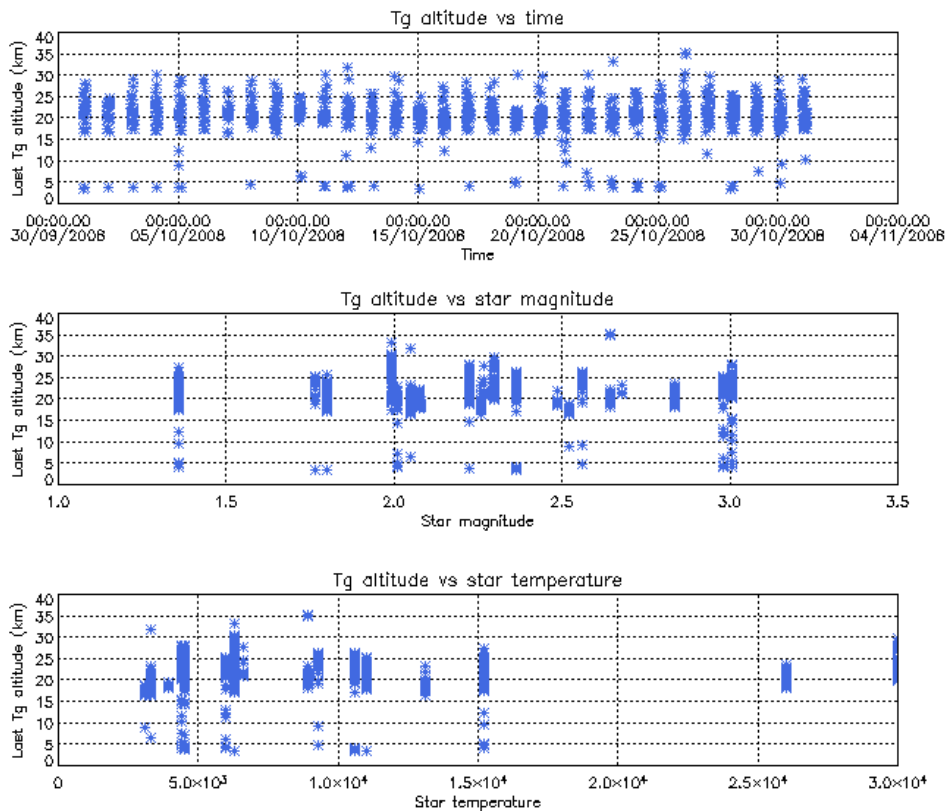


**Figure 4.6-4: Last tangent altitude of the occultation (bright limb), point at which the star is lost**

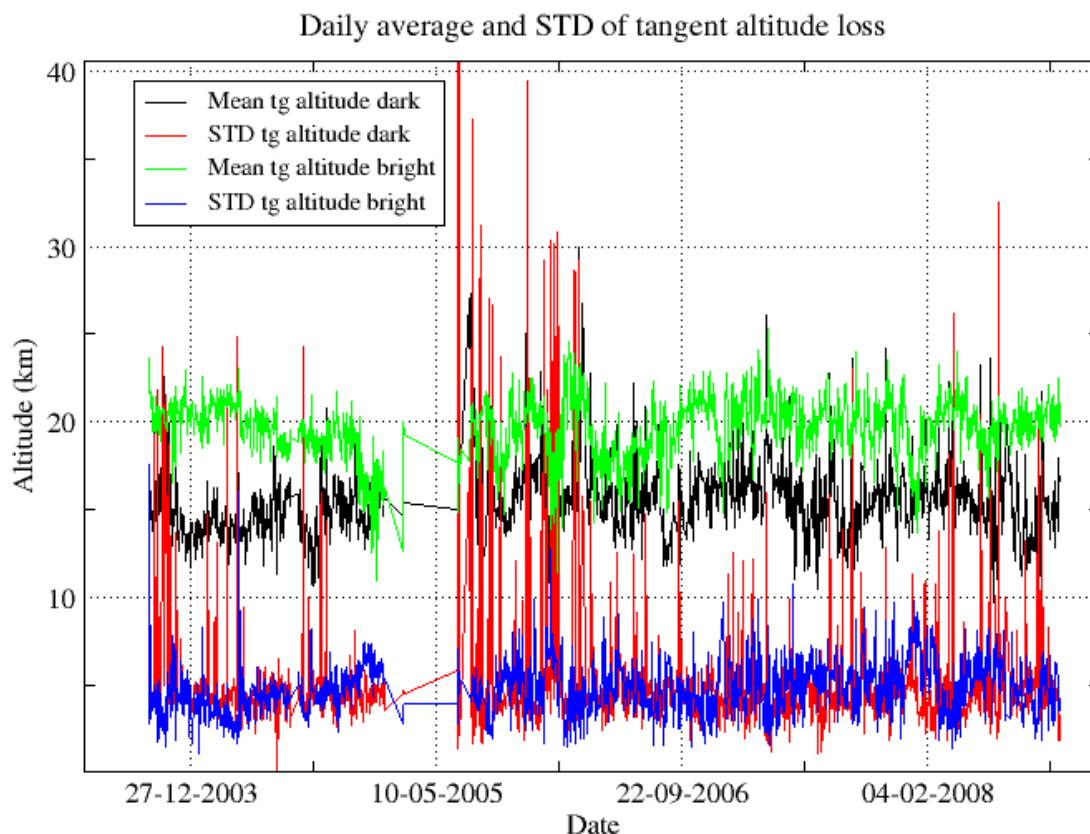


Figure 4.6-5: Daily average and STD of tangent altitude loss for the reporting period

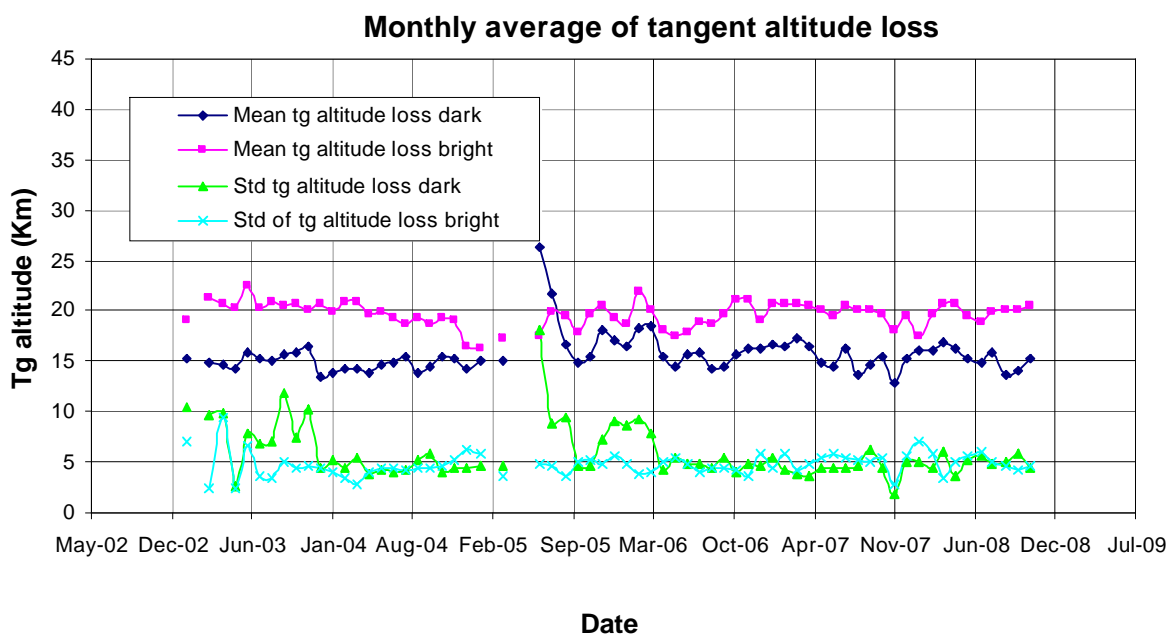


Figure 4.6-6: Monthly mean tangent altitude (and STD) at which the star is lost since January 2003

### 4.6.3 MOST ILLUMINATED PIXEL (MIP)

The MIP (Most Illuminated Pixel) is the star position on the SATU CCD in detection mode and it is recorded in the housekeeping data. The nominal centre of the SATU is pixel number **145** in elevation and number **205** in azimuth. The detection of the stars should not be far from this centre. As it can be seen in fig. 4.6-7 the **azimuth MIP** was within the threshold (table 4.6-1) since September 2002 until the occurrence of the anomaly on January 2005, even if a small variation is present. The reason for the change in trend observed after the anomaly is, at the moment, not understood. The **elevation MIP** had a significant variation (see the *note* below) until 12<sup>th</sup> December 2003 when a new PSO algorithm was activated in order to reduce the deviations of the ENVISAT platform attitude with respect to the nominal one. Similarly to the azimuth, after the anomaly of January 2005 the Elevation MIP has a drift that has no explanation. Investigations are ongoing to try to understand this behavior of the MIP as, although it does not impact the data quality or the star location on the CCD array during the measurements, it may invalidate attitude monitoring by GOMOS and could represent a hidden anomaly.

*Note:* A MIP variation onto the SATU CCD of 50 pixels corresponds to a de-pointing of 0.1 degrees

**Table 4-11: MIP Thresholds**

<b>MIP X</b>	<b>Mean delta Az</b>	[198 - 210]
	<b>Std delta Az</b>	7
<b>MIP Y</b>	<b>Mean delta El</b>	[140 – 150]
	<b>Std delta El</b>	4

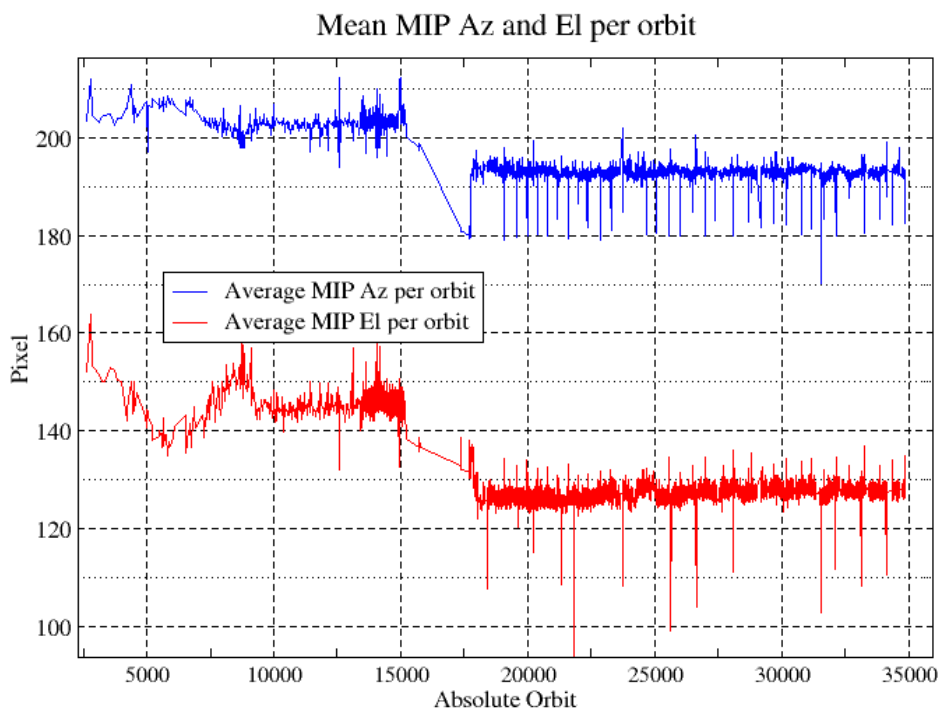


**Figure 4.6-7: Mean values of MIP for some orbits since 1<sup>st</sup> September 2002 (see table 4.6-1)**

Fig. 4.6-8 shows the standard deviation of azimuth and elevation MIP that should be within the thresholds of table 4.6-1. The peaks observed mean that one (or more) stars were detected very far from

the SATU detection point and, in this case, the stars were lost during the centering phase (see section 3.2 for stars lost in centering).

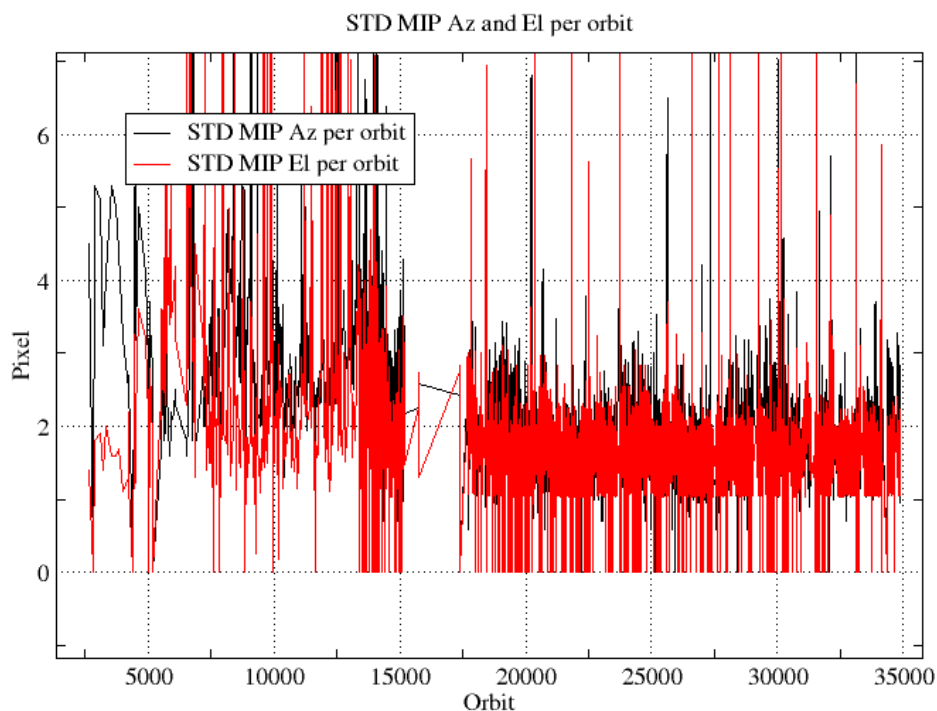


Figure 4.6-8: Standard deviation of MIP Azimuth and Elevation for some orbits since 1<sup>st</sup> September 2002 until end of reporting period (see table 4.6-1)

## 5 LEVEL 1 PRODUCT QUALITY MONITORING

### 5.1 Processor Configuration

#### 5.1.1 VERSION

Around 19% of near real time GOM\_TRA\_1P products have been received by the IDEAS team for routine quality control and long term trend quality monitoring. The current level 1-processor software version for the operational ground segment is GOMOS/5.00 since 8<sup>th</sup> August 2006 (see table 5.1-1). The product specification is PO-RS-MDA-GS2009\_10\_3I. This processor has been cleared for level 1 data release, with a disclaimer for known artefacts (<http://envisat.esa.int/dataproducts/availability/disclaimers>) that are currently being resolved and will be implemented in following releases of the processor (<http://envisat.esa.int/dataproducts/availability>).

Users are also supplied with 2002 - 4<sup>th</sup> July 2006 data sets reprocessed by the last prototype processor GOPR\_6.0c\_6.0f developed and operated by ACRI. See table 5.1-2 for prototype level 1b versions and modifications. The current GOMOS operational ground segment version GOMOS/5.00 is in line with the prototype version used for this second reprocessing.



**Table 5-1: PDS level 1b product version and main modifications implemented**

Date	Version	Description of changes
08-AUG-2006	Level 1b version 5.00 at PDHS-E, PDHS-K	Algorithm baseline level 1b DPM 6.3 <ul style="list-style-type: none"> <li>• Correction of FP unfolding algorithm</li> <li>• Background correction of SPB in full dark limb</li> <li>• Modification of the computation of the incidence angle</li> <li>• Correction of the flat-field correction equations</li> <li>• Star spectrum location on CCD modified for SPB</li> <li>• Provide SFA and SATU angles in degrees</li> <li>• Elevation angle dependency of the reflectivity LUT added in the algorithms</li> <li>• Ratio upper/star signal added (FLAGUC)</li> <li>• Add Dark Charge used for dark charge correction (per band)</li> <li>• Flag for illumination condition (PCDillum)</li> <li>• Minimum sample value for which the cosmic rays detection processing is applied (Crmin) is a function of gain index</li> <li>• Logic for computation of the flags attached to the reference star spectrum (Flref) modified</li> <li>• Add the computation of the sun direction in the inertial geocentric frame to be written in the level 1b and limb products.</li> <li>• Spectrometer effective sampling time added</li> </ul>
23-JUL-2006	Level 1b version 5.00 at LRAC	Change in configuration at the time of switch over: <ul style="list-style-type: none"> <li>○ Use of new reflectivity LUT (GOM_CAL_AX)</li> <li>○ New wavelength assignment for SPA1, A2, B1 (GOM_CAL_AX)</li> <li>○ Location of star spectrum projection on the CCD arrays (GOM_CAL_AX)</li> <li>○ Spatial PSF of SPB modified (GOM_INS_AX)</li> <li>○ Some universal constants (GOM_PR1_AX)</li> </ul>
23-MAR-2004	Level 1b version 4.02 at PDHS-E and PDHS-K	Algorithm baseline level 1b DPM 6.0 <ul style="list-style-type: none"> <li>• Adding a new calibration parameters (these values are hard coded at the moment)</li> <li>• Removal of redundancy chain from code</li> <li>• Modifications in the processing to apply new configuration and calibration parameter</li> <li>• New algorithm to determine between dark, twilight and bright limb and to handle data accordingly</li> <li>• Added handling of source packages with invalid packet header</li> <li>• Added enumerations for all configuration flags</li> </ul>
31-MAY-2003	Level 1b version 4.00 at PDHS-E and PDHS-K	Algorithm baseline level 1b DPM 5.4: <ul style="list-style-type: none"> <li>• Modulation correction step added after the cosmic rays detection processing</li> <li>• Inversion of the non-linearity and offset corrections</li> <li>• Modification of the computation of the estimated background signal measured by the photometers: use the spectrometer radiometric sensitivity curve and the photometer transfer function.</li> <li>• Use of the dark charge map at orbit level computed from the DSA (dark sky area) if any in the level 0 product</li> <li>• Implementation of a new unfolding algorithm for the photometer samples</li> </ul>
21-NOV-2002	Level 1b version 3.61 at PDHS-E and PDHS-K	Algorithm baseline DPM 5.3: <ul style="list-style-type: none"> <li>• Review of some default values</li> <li>• New definition of one PCD flag (atmosphere)</li> <li>• Temporal interpolation of ECMWF data</li> </ul>

**Table 5-2: GOPR level 1b product version and main modifications implemented**

Date	Version	Description of changes
22-JUL-2005	GOPR_6.0c	Level 1b: <ul style="list-style-type: none"> <li>• Correction of FP unfolding algorithm</li> <li>• Background correction of SPB in full dark limb</li> <li>• Modification of the computation of the incidence angle</li> <li>• Correction of the flat-field correction equations</li> <li>• Star spectrum location on CCD modified for SPB</li> </ul> Configuration for second reprocessing: <ul style="list-style-type: none"> <li>○ Use of new reflectivity LUT</li> <li>○ New wavelength assignment for SPA1, A2, B1</li> <li>○ Spatial PSF of SPB modified</li> </ul>
17-MAR-2004	GOPR 6.0a	<ul style="list-style-type: none"> <li>• Provide SFA and SATU angles in degrees</li> <li>• Elevation angle dependency of the reflectivity LUT added in the algorithms</li> <li>• Ratio upper/star signal added (FLAGUC)</li> <li>• Add Dark Charge used for dark charge correction (per band)</li> <li>• Flag for illumination condition (PCDillum)</li> <li>• Minimum sample value for which the cosmic rays detection processing is applied (Crmin) is a function of gain index</li> <li>• Logic for computation of the flags attached to the reference star spectrum (Flref) modified</li> <li>• Add the computation of the sun direction in the inertial geocentric frame to be written in the level 1b and limb products.</li> <li>• Spectrometer effective sampling time added</li> </ul>
25-JUL-2003	GOPR 5.4f	<ul style="list-style-type: none"> <li>• The demodulation process is applied only in full dark limb and twilight limb conditions.</li> </ul>
17-JUL-2003	GOPR 5.4e	<ul style="list-style-type: none"> <li>• Sun zenith angle is computed in the geolocation process. The occultation is now classified into (0) full dark limb condition, (1) bright limb condition and (2) twilight limb condition.</li> <li>• No background correction applied in full dark limb condition. The location of the image of the star spectrum on the CCD array is no more aligned with the CCD lines.</li> </ul>
02-JUL2003	GOPR 5.4d	<ul style="list-style-type: none"> <li>• The maximum number of measurements is set to 509 (instead of 510) in the GOPR prototype.</li> </ul>
17-MAR-2003	GOPR 5.4c	<ul style="list-style-type: none"> <li>• Modification of the CAL ADFs (update of the limb radiometric LUT). The products are affected only if the limb spectra are converted into physical units</li> <li>• Modifications to allow compatibility with ACRI computational cluster (no modifications of the results)</li> <li>• Modification of the logic to handle dark charge map refresh at orbit level (DSA data is now directly processed by the level 1b processor if available in the level 0 product). No impact on the results</li> </ul>
21-FEB-2003	GOPR 5.4b	<ul style="list-style-type: none"> <li>• DC map values are rounded when written in the level 1b product</li> <li>• Modification of the CAL ADFs (update of the wavelength assignment of SPB1 and SPB2)</li> <li>• Modify the computation of flag_mod in the modulation correction routine</li> </ul>
17-JAN-2003	GOPR 5.4a	<ul style="list-style-type: none"> <li>• use the start and stop dates of the occultation when calling the CFI Interpol instead of start and stop dates of the level 0 product</li> <li>• modify the ECMWF filename information in the SPH of the level 1b and limb products</li> </ul>

### 5.1.2 AUXILIARY DATA FILES (ADF)

The ADF's files in tables 5.1-3, 5.1-4, 5.1-5, 5.1-6 and 5.1-7 have been disseminated to the PDS during the whole mission. Note that the files outlined in yellow are the set of auxiliary files used during the reporting period. For every type of file, the validity runs from the start validity time until the start validity time of the following one, but if an ADF file has been disseminated after the start validity time, it is obvious that it will be used by the PDHS-E and PDHS-K PDS only after the dissemination time (this happens the majority of the time). Just like the other ADF's, the calibration auxiliary file (GOM\_CAL\_AX) has been updated several times in the past (table 5.1-7) but the difference is that now it is updated in a weekly basis with new DC maps and new wavelength assignment (routine weekly wavelength calibration was activated on 14<sup>th</sup> December 2007), and that is why the files used during reporting period are reported in a separate table (table 5.1-8) that changes from report to report.

**Table 5-3: Historic GOM\_PR1\_AX files used by PDS for level 1b products generation. The GOM\_PR1\_AX is a file containing the configuration parameters used for processing from level 0 to level 1b products**

Used by PDS for Level 1b products generation during	GOM_PR1_AX (GOMOS processing level 1b configuration file)
01-MAR-2002 → 29-MAR-2002	GOM_PR1_AXVIEC20020121_165314_20020101_000000_20200101_000000 <ul style="list-style-type: none"> <li>• Pre-launch configuration</li> </ul>
30-MAR-2002 → 14-NOV-2002	GOM_PR1_AXVIEC20020329_115921_20020324_200000_20100101_000000 <ul style="list-style-type: none"> <li>• Changed num_grid_upper, thr_conv and max_iter in the atmospheric GADS</li> </ul>
Not used	GOM_PR1_AXVIEC20020729_083756_20020301_000000_20100101_000000 <ul style="list-style-type: none"> <li>• Cosmic Ray mode + threshold</li> <li>• DC correction based on maps</li> <li>• Non-linearity correction disabled</li> </ul>
Not used	GOM_PR1_AXVIEC20021112_170331_20020301_000000_20100101_000000 <ul style="list-style-type: none"> <li>• Central background estimation by linear interpolation + associated thresholds</li> </ul>
15-NOV-2002 → 26-MAR-2003	GOM_PR1_AXVIEC20021114_153119_20020324_000000_20100101_000000 <ul style="list-style-type: none"> <li>• Same content as GOM_PR1_AXVIEC20021112_170331_20020301_000000_20100101_000000 but validity start updated so as to supersede according to the PDS file selection rules</li> </ul>
27-MAR-2003 → 19-MAR-2004	GOM_PR1_AXVIEC20030326_085805_20020324_200000_20100101_000000 <ul style="list-style-type: none"> <li>• Same content as GOM_PR1_AXVIEC20021112_170331_20020301_000000_20100101_000000 but validity start updated so as to supersede according to the PDS file selection rules</li> </ul>
20-MAR-2004 → 22-MAR-2004	GOM_PR1_AXVIEC20040319_134932_20020324_200000_20100101_000000 <ul style="list-style-type: none"> <li>• Ray tracing parameter changed: convergence criteria set to 0.1 microrad</li> </ul>
23-MAR-2004 → 01-APR-2004 <i>Notes:</i> <ul style="list-style-type: none"> <li>• This file was constructed from GOM_PR1_AXVIEC20030326_085805_20020324_200000_20100101_000000 (so without the ray tracing parameter changed)</li> </ul>	GOM_PR1_AXVIEC20040316_144850_20020324_200000_20100101_000000 GOM_PR1 ADF for version GOMOS/4.02, changes: <ul style="list-style-type: none"> <li>• The central band estimation mode</li> <li>• Atmosphere thickness</li> <li>• Altitude discretisation</li> </ul>

<ul style="list-style-type: none"> <li>This file was used by the GOMOS/4.02 processors before the IECF dissemination. The dissemination was done on 25<sup>th</sup> March 2004</li> </ul>	
02-APR-2004 → 07-AUG-2006	GOM_PR1_AXVIEC20040401_083133_20020324_200000_20100101_000000 <ul style="list-style-type: none"> <li>Ray tracing parameter changed: convergence criteria set to 0.1 microrad</li> </ul>
08-AUG-2006 Used at the time of switching over GOMOS/5.00	GOM_PR1_AXNIEC20050627_151042_20020301_000000_20100101_000000 <ul style="list-style-type: none"> <li>Change of some universal constants</li> </ul>

**Table 5-4: Historic GOM\_INS\_AX files used by PDS for level 1b products generation. The GOM\_INS\_AX is a file containing the characteristics of the instrument and it is used for processing from level 0 to level 1b products and from level 1b to level 2 products**

Used by PDS for Level 1b products generation during	GOM_INS_AX (GOMOS instrument characteristics file)
01-MAR-2002 → 29-JUL-2002	GOM_INS_AXVIEC20020121_165107_20020101_000000_20200101_000000 <ul style="list-style-type: none"> <li>Pre-launch configuration</li> </ul>
30-JUL-2002 → 12-NOV-2002	GOM_INS_AXVIEC20020729_083625_20020301_000000_20100101_000000 <ul style="list-style-type: none"> <li>Factors for the conversion of the SFA angles from SFM axes to GOMOS axes</li> </ul>
13-NOV-2002 → 16-JUL-2003	GOM_INS_AXVIEC20021112_170146_20020301_000000_20100101_000000 <ul style="list-style-type: none"> <li>No more invalid spectral range</li> </ul>
Not used	GOM_INS_AXVIEC20030716_080112_20030711_120000_20100101_000000 <ul style="list-style-type: none"> <li>New value for SFM elevation zero offset for redundant chain: 10004</li> </ul>
17-JUL-2003 → 07-AUG-2006	GOM_INS_AXVIEC20030716_105425_20030716_120000_20100101_000000 <ul style="list-style-type: none"> <li>Bias induct azimuth redundant value set to -0.0084 rad (-0.4813 deg)</li> </ul>
08-AUG-2006 Used at the time of switching over GOMOS/5.00	GOM_INS_AXNIEC20050627_150713_20030716_120000_20100101_000000 <ul style="list-style-type: none"> <li>The spatial PSF of SPB</li> </ul>

**Table 5-5: Historic GOM\_CAT\_AX files used by PDS for level 1b products generation. The GOM\_CAT\_AX is a file holding the star catalogue used for processing from level 0 to level 1b products**

Used by PDS for Level 1b products generation during	GOM_CAT_AX (GOMOS Stat Catalogue file)
01-MAR-2002	GOM_CAT_AXVIEC20020121_161009_20020101_000000_20200101_000000 <ul style="list-style-type: none"> <li>Pre-launch configuration</li> </ul>

**Table 5-6: Historic GOM\_STS\_AX files used by PDS for level 1b products generation. The GOM\_STS\_AX is a file containing star spectra used for processing from level 0 to level 1b products**

Used by PDS for Level 1b products generation during	GOM_STS_AX (GOMOS Star Spectra file)
01-MAR-2002 → 07-AUG-2006	GOM_STS_AXVIEC20020121_165822_20020101_000000_20200101_000000 <ul style="list-style-type: none"> <li>Pre-launch configuration</li> </ul>
08-AUG-2006 Used at the time of switching over GOMOS/5.00	GOM_STS_AXNIEC20040308_103538_20020101_160000_20100101_000000 <ul style="list-style-type: none"> <li>Wavelength assignment GADS has been suppressed from the product</li> <li>Wavelength assignment vector has been added to the star spectrum</li> </ul>

**Table 5-7: Historic GOM\_CAL\_AX files used by PDS for level 1b products generation. The GOM\_CAL\_AX is a file containing the calibration parameters used for processing from level 0 to level 1b products**

Used by PDS for Level 1b products generation during	GOM_CAL_AX (GOMOS Calibration file)
01-MAR-2002 → 29-JUL-2002	GOM_CAL_AXVIEC20020121_164808_20020101_000000_20200101_000000 <ul style="list-style-type: none"> <li>• Pre-launch configuration</li> </ul>
Not used	GOM_CAL_AXVIEC20020121_142519_20020101_000000_20200101_000000 <ul style="list-style-type: none"> <li>• Pre-launch configuration</li> </ul>
30-JUL-2002 → 12-NOV-2002	GOM_CAL_AXVIEC20020729_082426_20020717_193500_20100101_000000 <ul style="list-style-type: none"> <li>• Band setting information</li> <li>• Wavelength assignment</li> <li>• Spectral dispersion LUT</li> <li>• ADC offset for Spectrometers</li> <li>• PRNU maps</li> <li>• Thermistor coding LUT</li> <li>• DC maps</li> </ul>
Not used	GOM_CAL_AXVIEC20021112_165603_20020914_000000_20100101_000000 <ul style="list-style-type: none"> <li>• Band setting information</li> <li>• DC maps</li> <li>• PRNU maps</li> <li>• Wavelength assignment</li> <li>• Spectral dispersion LUT</li> <li>• Radiometric sensitivity LUT (star and limb)</li> <li>• SP-FP intercalibration LUT</li> <li>• Vignetting LUT</li> <li>• Reflectivity LUT</li> <li>• ADC offset</li> </ul>
13-NOV-2002 → 30-JAN-2003	GOM_CAL_AXVIEC20021112_165948_20021019_000000_20100101_000000 <ul style="list-style-type: none"> <li>• Only DC maps updated</li> </ul>
31-JAN-2003 → 11-APR-2003	GOM_CAL_AXVIEC20030130_133032_20030101_000000_20100101_000000 <ul style="list-style-type: none"> <li>• Only DC maps updated (using DSA of orbit 04541)</li> </ul>
12-APR-2003 → 02-JUN-2003	GOM_CAL_AXVIEC20030411_065739_20030407_000000_20100101_000000 <ul style="list-style-type: none"> <li>• Modification of the radiometric sensitivity curve for the limb spectra. Note that the modification of this LUT has no impact on the GOMOS processing. The LUT is just copied into the level 1b limb product for user conversion purpose.</li> <li>• Updated DC map only (using DSA of orbit 05762).</li> </ul>
03-JUN-2003: from this date onwards, mainly updates to DC maps are done. Every month, the table of new GOM_CAL files with <b>only</b> DC maps updated is provided (table 5.1-8). Eventual changes to this file not corresponding only to DC maps updates will be reported in this table.	GOM_CAL_AXVIEC20030602_094748_20030531_000000_20100101_000000 <ul style="list-style-type: none"> <li>• Updated DC maps only (using DSA of orbit 06530)</li> </ul>
13-FEB-2004 → 23-FEB-2004	GOM_CAL_AXVIEC20040212_103916_20040209_000000_20100101_000000 <ul style="list-style-type: none"> <li>• Update of the reflectivity LUT</li> <li>• Updated DC maps (Orbit 10194, date 11-FEB-2004)</li> </ul>
08-AUG-2006 Used at the time of switching over GOMOS/5.00	GOM_CAL_AXNIEC20050704_110915_20050125_224800_20100101_000000 <ul style="list-style-type: none"> <li>• Reflectivity LUT updated</li> <li>• Location of the star spectrum projection on the CCD arrays</li> <li>• Wavelength assignment of the spectra updated</li> <li>• The spatial LSF of SPB updated</li> <li>• Updated DC maps (orbit 15200, date 25 JAN 2005)</li> </ul>

**Table 5-8: Calibration ADF for reporting period. These files are updated (only with DC maps) in a 8-10 days basis**

Used by PDS for Level 1b products generation during	GOM_CAL_AX (GOMOS Calibration file)
30-SEP-2008 → 08-OCT-2008	GOM_CAL_AXVIEC20080929_142519_20080927_000000_20100101_000000 (date 28 SEP 2008, orbit 34406)
09-OCT-2008 → 16-OCT-2008	GOM_CAL_AXVIEC20081008_081911_20081006_000000_20100101_000000 (orbit 34536, date 07 OCT 2008)
17-OCT-2008 → 03-NOV-2008	GOM_CAL_AXVIEC20081016_095516_20081014_000000_20100101_000000 (orbit 34648, date 15 OCT 2008)

## 5.2 Quality Flags Monitoring

In this section, the results of monitoring some Product Quality information stored in level 1b products that did not have a fatal error (MPH error flag not set) are discussed. The products with fatal errors were around 0.4% of the products received during the reporting month for the quality monitoring.

On the one hand, for every product we have information of the **number of measurements** where a given problem was detected (i.e. number of invalid measurements, number of measurements containing saturated samples, number of measurements with demodulation flag set...). On the other hand, there are **flags** that indicate problems within the product (i.e. flag set to one if the reference spectrum was computed from DB, flag set to zero if SATU data were not used...).

For the information on the number of measurements a plot of percentages with respect to time is provided in fig. 5.2-1. The most relevant part of this information is also plotted in a world map as a function of ENVISAT position: % of cosmic ray hits per profile, % of datation errors per profile, % of star falling outside the central band per profile and % of saturation errors per profile (fig.5-2.2a).

It can be seen from fig. 5.2-1 that the cosmic rays hits occurred several times for the 99% of the measurements of the products. Looking at fig. 5.2-2a it can be clearly observed that this high percentage occurred when the satellite crossed the South Atlantic Anomaly (SAA) zone. Also the percentage of saturation errors per profile shows an increase over the SAA zone.

Another observation from fig. 5.2-1 is that for several products, 30-35% of the measurements have the star signal falling outside the central band. In fig. 5.2-2a it is observed that this percentage occurred mainly during twilight/dark conditions (roughly ascending) while in bright conditions the percentage is around 10% (fig.5.2-2a). This is because during the night the stars are lost deeper within the atmosphere and the turbulence phenomena becomes more important, producing the star to be less ‘focused’ on the spectrometers central band.

The other values (% of invalid measurements per product, % of measurements per product with datation errors...) are quite low.

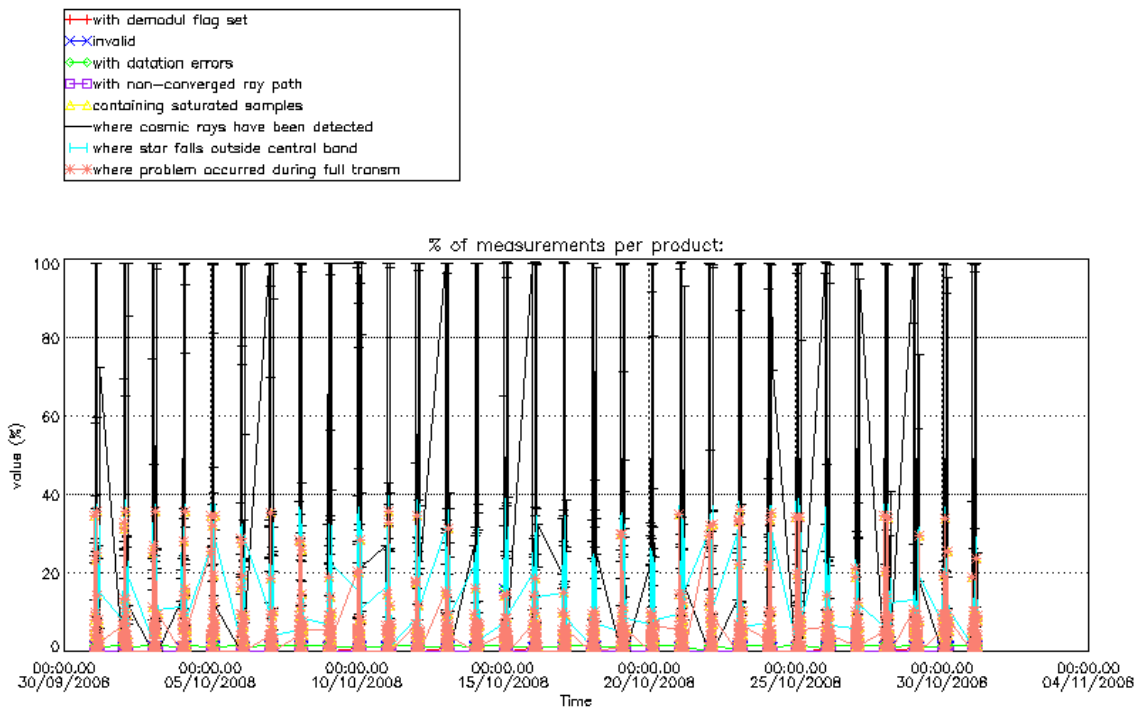


Figure 5.2-1: Level 1b product quality monitoring with respect to time

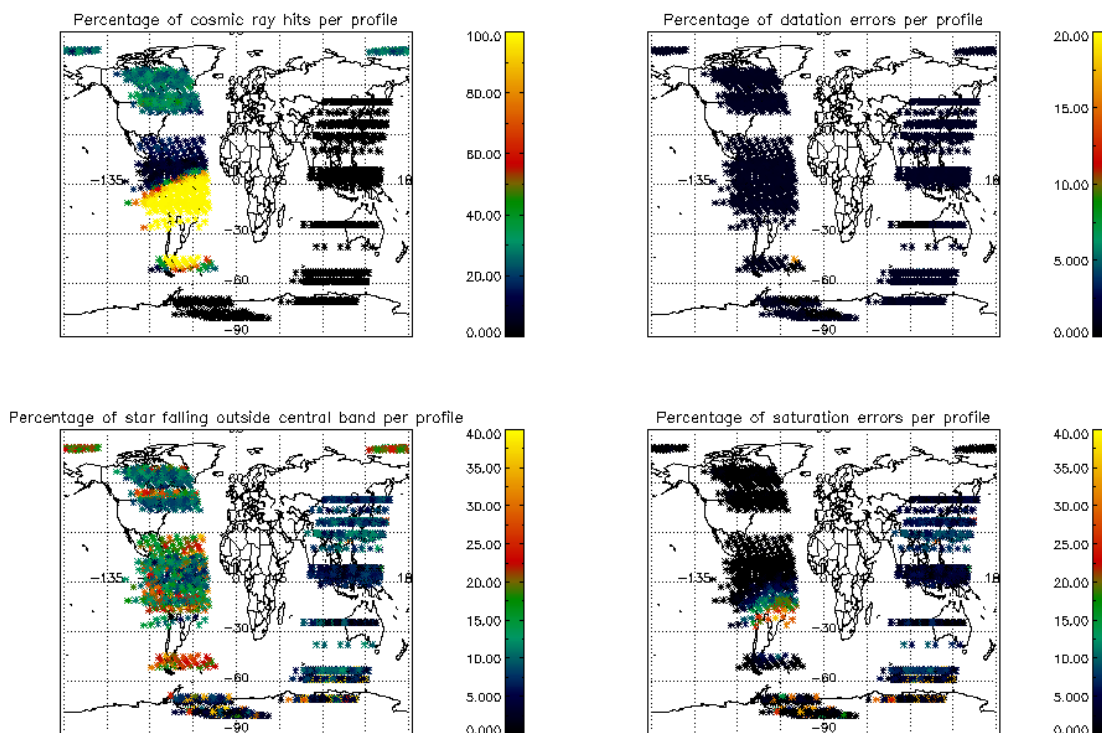
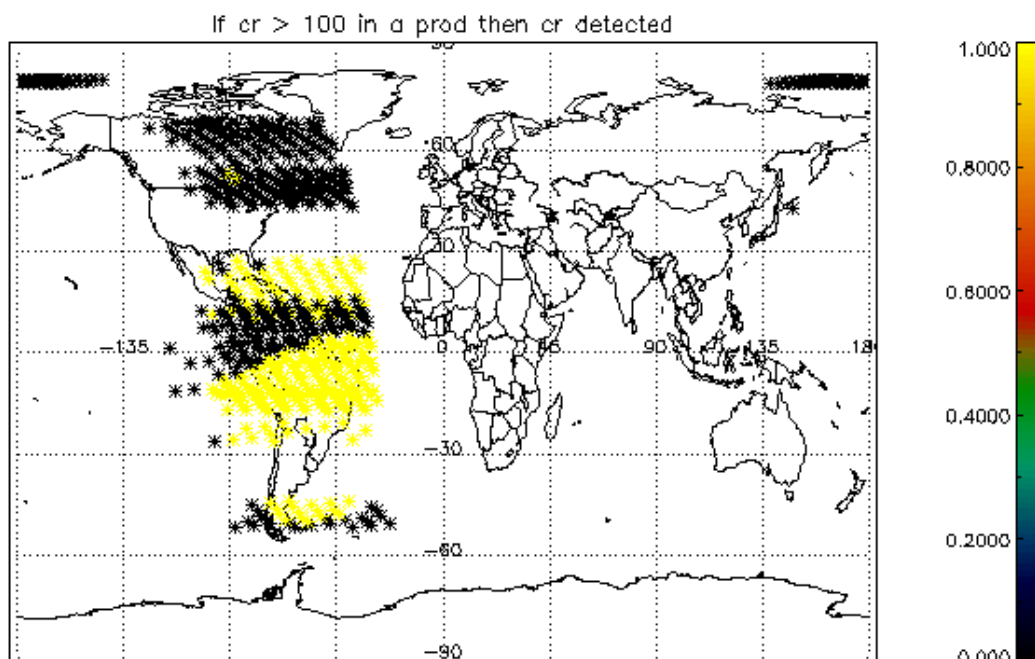


Figure 5.2-2a: Level 1b product quality monitoring with respect to geolocation of ENVISAT

The QWG has requested to perform a different plot of the cosmic rays in order to have a clear picture on the geographical position of the hits: count the cosmic rays detected in every product and when they are more that 100 then consider that cosmic rays have been detected. This plot is in fig. 5.2-2b. The products

in bright limb have not been considered because the cosmic rays detection is not activated when processing products in bright.



**Figure 5.2-2b: Count every time a cosmic ray has been detected. When it is > 100, then cosmic rays detected (yellow in the plot)**

The flag information is given in table 5.2-1. The percentage of the products that have at least one measurement with demodulation flag set is also reported.

**Table 5-9: Percentage of products during the reporting period with:**

At least one measurement with demodulation flag set:	35 %
Reference spectrum computed from DB:	0.0 %
Reference spectrum with small number of measurements:	0.0 %
SATU data not used:	0.0 %

### 5.2.1 QUALITY FLAGS MONITORING (EXTRACTED FROM LEVEL 2 PRODUCTS)

In this section, the Product Quality information coming from the level 1 processing that is also stored in the level 2 products is plotted. Only products that did not have a fatal error (MPH error flag not set) are considered. The purpose of using the level 2 data is simply that the percentage of level 2 products arriving to the IDEAS team for the quality monitoring is much higher. For the reporting month, 98% of the archived products have been received. The plots are very similar to fig. 5.2-1 and 5.2-2a (demodulation flag information is not included) but separating ascending from descending passes. Since new version of the processor (GOMOS/5.00) there is no correspondence between illumination condition and latitude range when separating the passages (ascending and descending). Now, in the geo-location process, the sun zenith angle is computed and the occultation is then flagged accordingly (dark, bright,



twilight, straylight, twilight+straylight). You can see in fig. 5.2-3 the location of the occultations and their limb for the reporting month.

Fig. 5.2-4 and 5.2-5 present some quality information as a function of the time whereas in fig. 5.2-6 and 5.2-7 the plot is respect to the satellite position at the beginning of the occultations.

The percentage of measurements “where a problem occurred during the full transmission” per product ranges between 2 and 40 % (fig. 5.2-4, 5.2-5). The high values are due to the saturation that occurs mainly in bright limb. In dark limb the saturation occurs over the SAA zone but it is quite low elsewhere. From fig. 5.2-4 and 5.2-5 you can see also that there are a variable percentage of the measurements that have the star signal falling outside the central band. This is because in dark the stars are lost deeper within the atmosphere and the turbulence phenomena become more important, resulting in the star being less ‘focused’ on the spectrometers central band.

In ascending (fig. 5.2-6) the SAA is perfectly localized by the high percentage of cosmic ray hits per product (upper left panel). It is not the same if we look at fig. 5.2-7, because in descending most of the occultations in that world region are in bright limb conditions and the cosmic rays detection processing is not activated.

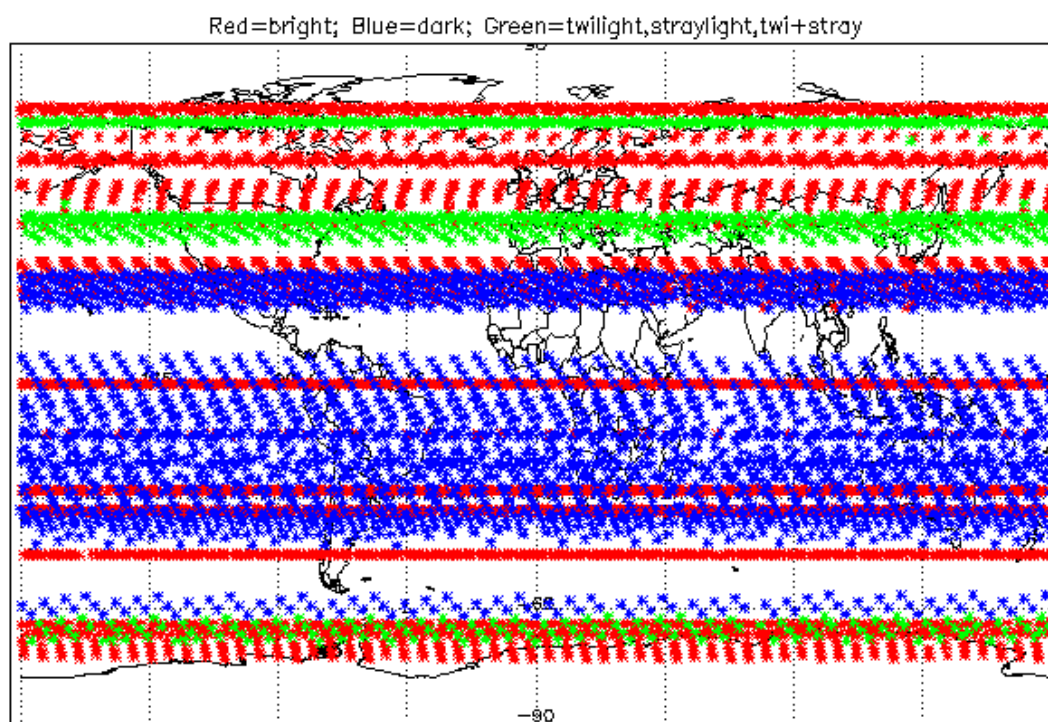


Figure 5.2-3: Position of the occultations based on illumination conditions

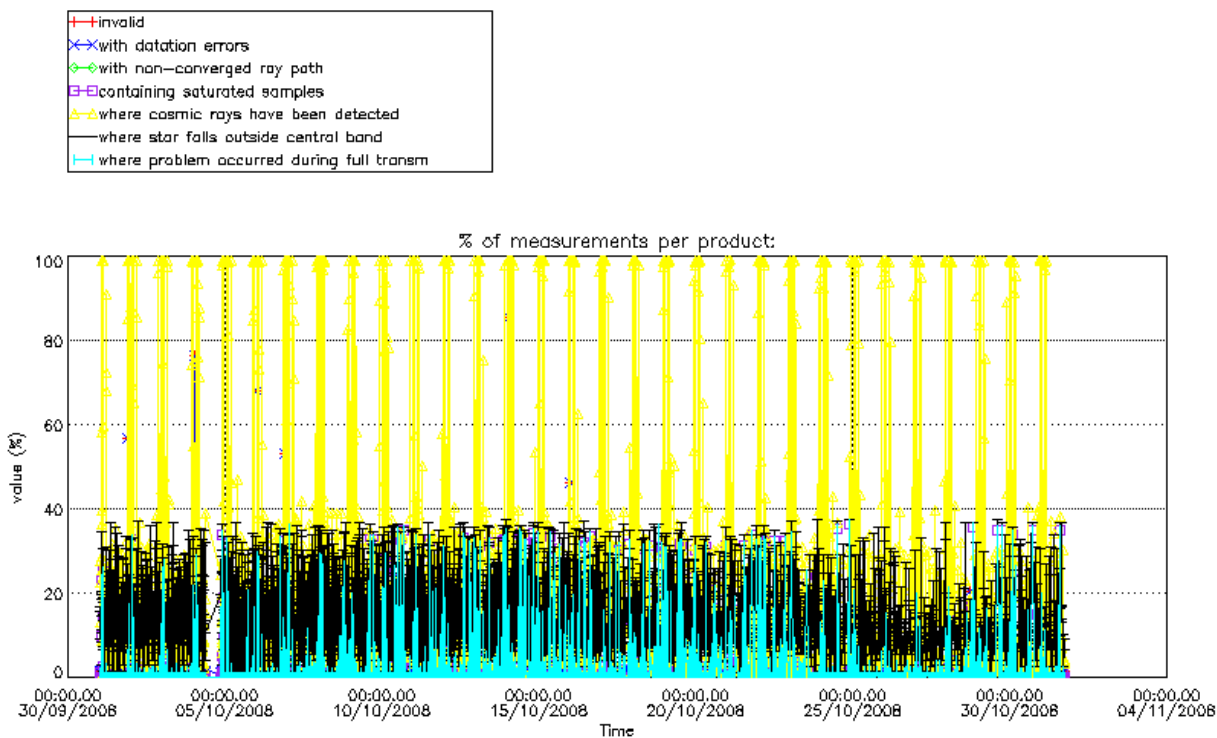


Figure 5.2-4: Level 1b product quality monitoring with respect to time ASCENDING ENVISAT passes

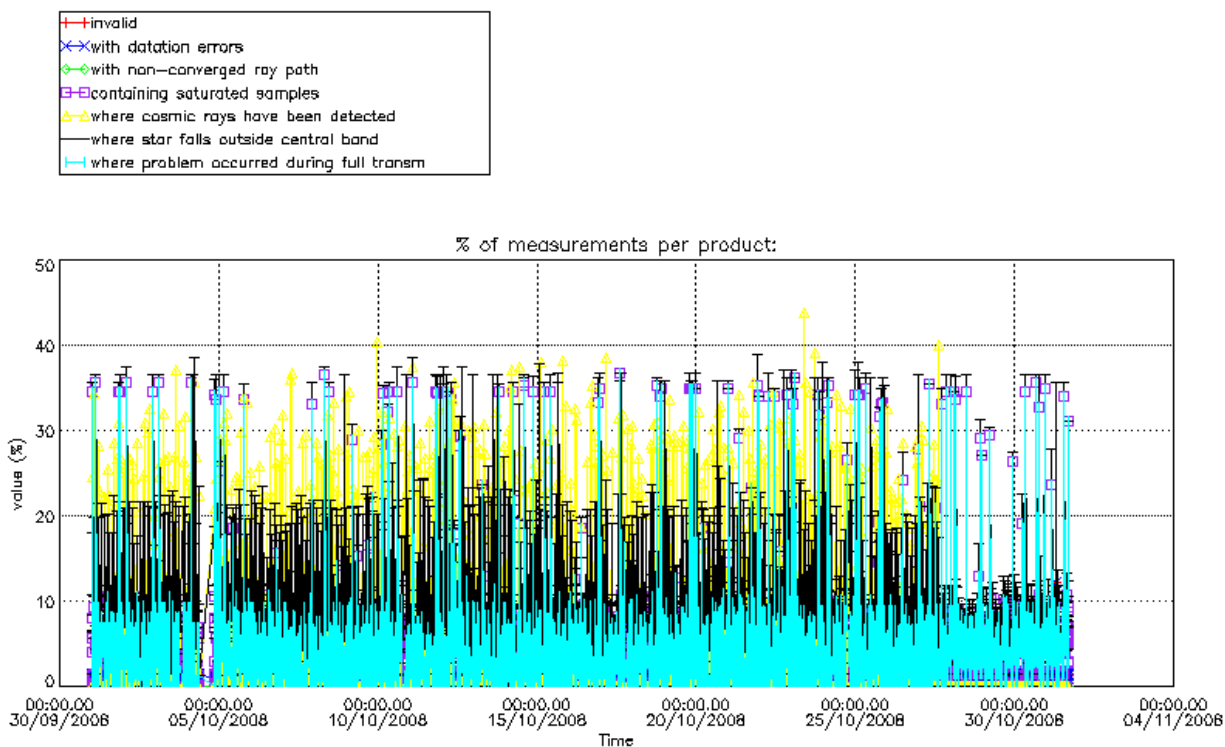
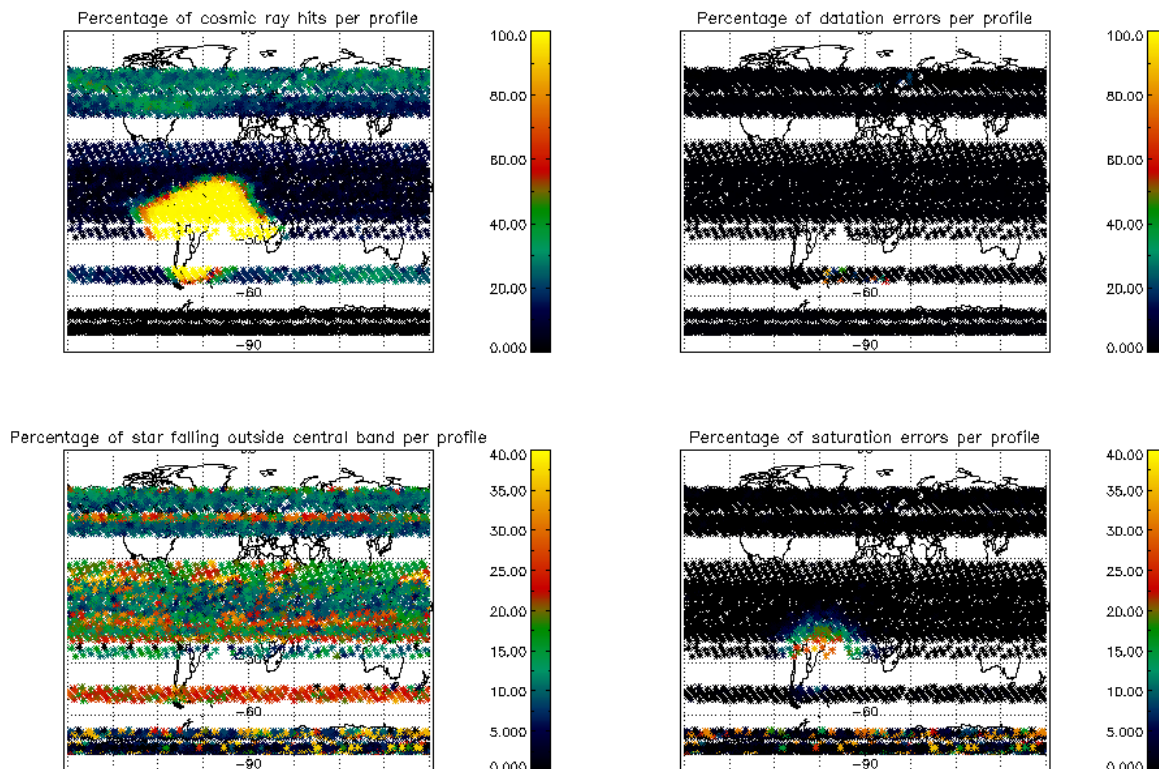
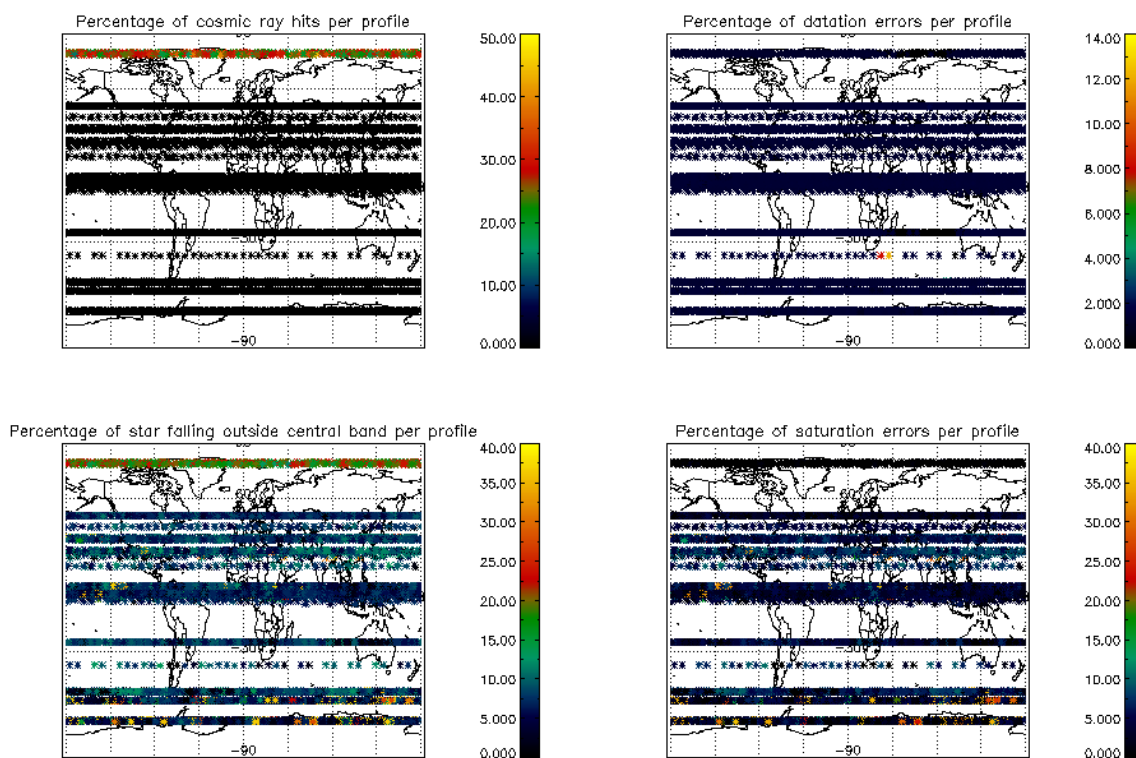


Figure 5.2-5: Level 1b product quality monitoring with respect to time DESCENDING ENVISAT passes



**Figure 5.2-6: Level 1b product quality monitoring with respect to satellite geo-location for ASCENDING ENVISAT passes**



**Figure 5.2-7: Level 1b product quality monitoring with respect to satellite geo-location for DESCENDING ENVISAT passes**

### 5.3 Spectral Performance

Every pixel of the spectrometers has a wavelength assigned. This assignment has been monitored through the mission by calculating, for given stars, the spectral shift corresponding to a maximum correlation between the reference star spectrum and the one of the occultation.

In order to have the wavelength well calibrated during the second reprocessing activity, the QWG performed a study to correct the spectral shift that was detected during the routine spectral performance monitoring (see fig. 5.3-1). A linear regression using data from stars 1 and 2 has been used to calibrate the wavelength for each needed orbit (one value for each calibration ADF used for the second reprocessing). This linear law took into account the ageing of the instrument. During the QWG #13, it has been decided to perform a wavelength calibration routinely with an extrapolation of this law and introducing also an extension to a second order law taking into account the seasonal variations. This routine calibration has been implemented on 14<sup>th</sup> December 2007 and is performed once a week at the same time of the DC maps calibration.

With this implementation the monitoring curve presented in fig. 5.3-1 (updated every month) should show small wavelength shifts since 14<sup>th</sup> December 2007. At least, the values should be smaller than the warning value set to 0.07 nm. This month, similarly to September 2008, the values are higher than 0.08 nm which is something not expected after the implementation of the routine calibration. The QWG has been informed and is investigating this issue.

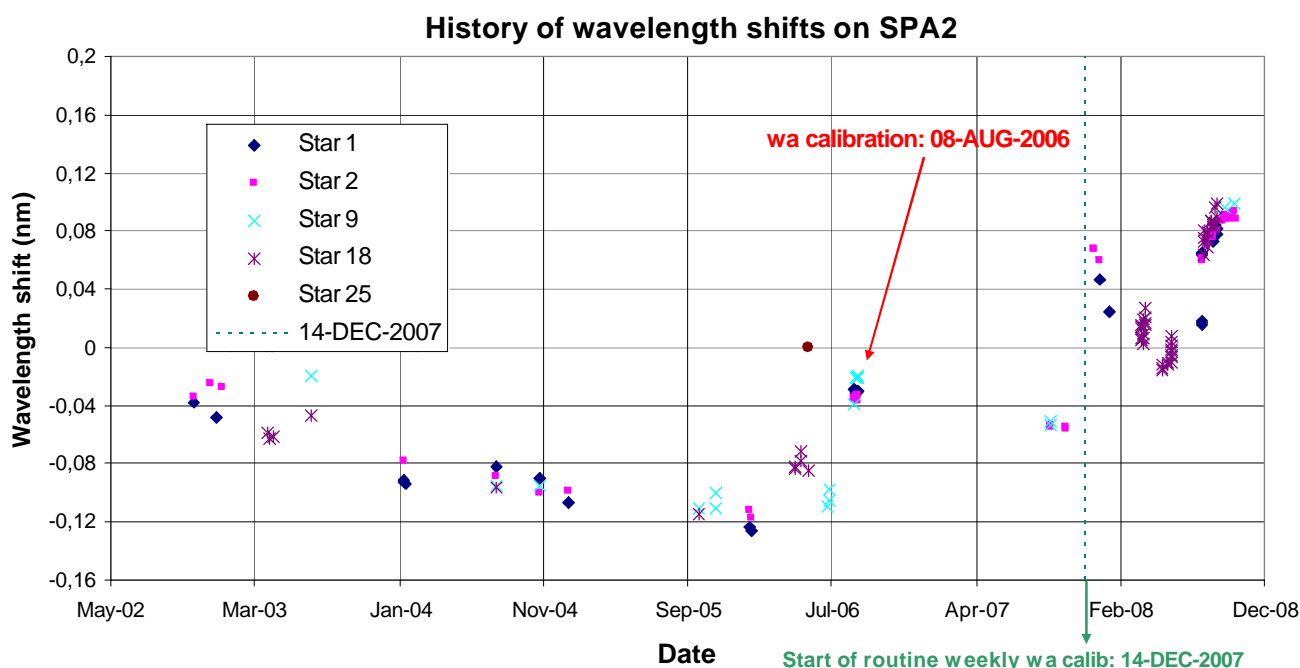


Figure 5.3-1: SPA2 wavelength monitoring since 12<sup>th</sup> November 2002: for every star ID (1, 2, 9, 18, 25) it is plotted the spectral shift for which a maximum correlation has been found between the reference spectrum and the one of the occultation

## 5.4 Radiometric Performance

### 5.4.1 RADIOMETRIC SENSITIVITY

The monitoring performed consists of the calculation of the radiometric sensitivity of each CCD by computing the ratio between parts of the reference spectrum using specific stars (fig. 5.4-1).

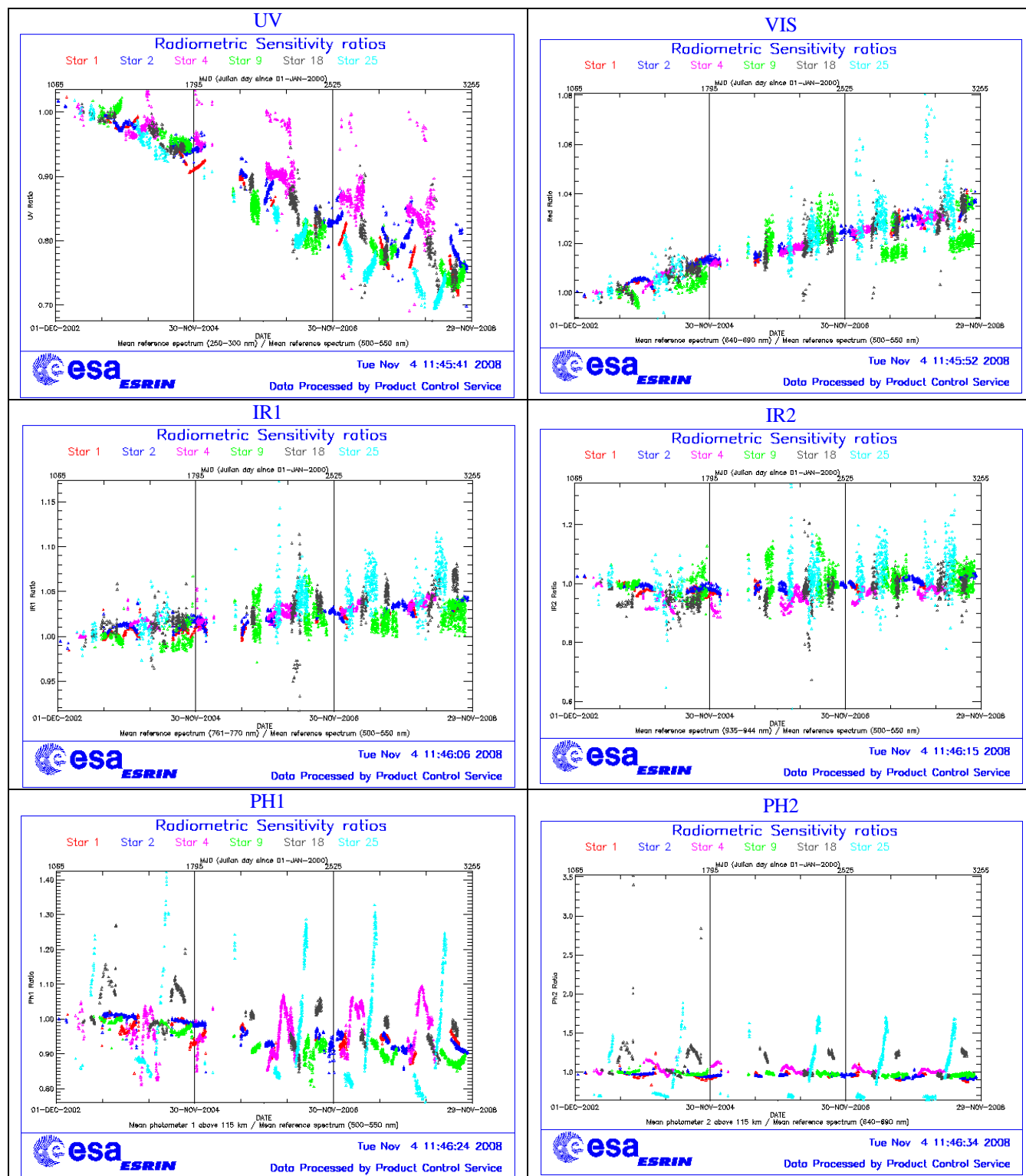


Figure 5.4-1: Radiometric sensitivity ratios since December 2002

The parts of the spectrum used are:

- UV: 250–300 nm;
- Yellow: 500–550 nm
- Red: 640–690 nm
- Ir1: 761-770 nm
- Ir2: 935-944 nm

For the spectrometers the ratios are with respect to the ‘yellow’ spectral range. For the photometers, the ratios are calculated by dividing the mean photometer signal above the atmosphere (115 km) by the ‘yellow’ spectral range (for PH1) or by the ‘red’ spectral range (for PH2). The variation of the ratio should be within a given threshold which is set to 10% (see table 5.4-1 that corresponds to fig. 5.4-1). For every star, this variation is calculated as the difference between the maximum (or minimum) ratio, and the mean over the 15 first values (if there were not 15 values computed yet, all values would be used).

**Table 5-10: Variation of RS for the different ratios (corresponds to fig. 5.4-1). Should be less than 10%**

Star Id	% Variation of UV ratio	% Variation of Red ratio	% Variation of IR1 ratio	% Variation of IR2 ratio	% Variation of Ph1 ratio	% Variation of Ph2 ratio
1	6.2	1.4	0.5	0.2	8.5	30.2
2	1.6	1.8	0.7	0.4	8.4	12.4
4	0.8	2.1	1.5	1.3	8.1	23.5
9	20.8	1.4	0.8	0.6	11.1	9.2
18	4.5	2.0	1.6	1.8	14.8	300.0
25	42.5	2.5	1.8	1.4	28.1	147.4

For star 9 and 25 the UV ratio is greater than the threshold 10%. It is clear (fig. 5.4-1) that there is a global decrease of UV ratios for all the stars. This confirms the expected degradation suffered by the UV optics that is, anyway, very small considering also the small variation for the rest of the stars (table 5.4-1).

By looking at the photometers radiometric sensitivity ratios of fig. 5.4-1, it can be seen that every star has a variation that seems to be annual. The variation is significant for stars 25 and 18. After some investigations performed by the QWG that exclude an inaccurate reflectivity correction LUT, it seems that the PH1/2 radiometric sensitivity variations could come from the fact that the spectrometers and the photometers are not illuminated the same way when the straylight appears (seasonal effect).

#### 5.4.2 PIXEL RESPONSE NON UNIFORMITY

No new PRNU calibration has been performed during the reporting period. This means that the PRNU maps inside the ADF remain as they are without any change for the moment.

### 5.5 Other Calibration Results

Future reports will address other calibration results, when available.

## 6 LEVEL 2 PRODUCT QUALITY MONITORING

### 6.1 Processor Configuration

#### 6.1.1 VERSION

Level 2 products from the operational ground segment have been disseminated during the reporting period to the users. Around 98% of GOM\_NL\_\_2P products have been received by the IDEAS team for routine quality control and long term trend monitoring. The current level 2-processor software version for the operational ground segment is GOMOS/5.00 since 8<sup>th</sup> August 2006 (see table 6.1-1). The product specification is PO-RS-MDA-GS2009\_10\_3I. Users are also supplied with 2002 - 4<sup>th</sup> July 2006 data sets reprocessed by the last prototype processor GOPR\_6.0c\_6.0f (developed and operated by ACRI) which is in line with the current GOMOS operational ground segment version GOMOS/5.00

**Table 6-1: PDS level 2 product version and main modifications implemented**

Date	Version	Description of changes
08-AUG-2006	Level 2 version 5.00 at PDHS-E and PDHS-K	Algorithm baseline level 2 DPM 6.2: <ul style="list-style-type: none"> <li>• The optimisation of the DOAS iterations</li> <li>• Negative column densities and local densities not flagged anymore</li> <li>• Suppress the setting of maximum error in case of negative local densities</li> <li>• Correction of HRTP discrepancies, and error estimates fixed</li> <li>• Rename Turbulence MDS into High Resolution Temperature MDS (HRTP)</li> <li>• Add vertical resolution per species in local densities MDS</li> <li>• Add Solar zenith angle at tangent point and at satellite level in geolocation ADS</li> <li>• Add "tangent point density from external model" in geolocation ADS</li> <li>• Suppress contribution of "tangent point density from external model" in "local air density from GOMOS atmospheric profile" in geolocation ADS</li> </ul>
23-JUL-2006	Level 2 version 5.00 at FinCoPAC	Change in configuration at the time of the switch over: <ul style="list-style-type: none"> <li>○ 2<sup>nd</sup> order polynomial for aerosol</li> <li>○ Air fixed to ECMWF (local density set to 0 in the L2 products)</li> <li>○ Orphal cross-sections for O<sub>3</sub></li> <li>○ GOMOS cross-sections for other species</li> <li>○ Covariance matrix terms linked to air set to 0</li> <li>○ Air and NO<sub>2</sub> additional errors set to 0</li> </ul>
23-MAR-2003	Level 2 version 4.02 at PDHS-E and PDHS-K	Algorithm baseline level 2 DPM 5.5: Section 3 <ul style="list-style-type: none"> <li>• Add references to technical notes on Tikhonov regularization</li> <li>• Change High level breakdown of modules:</li> </ul>

		<p>SMO/PFG</p> <ul style="list-style-type: none"> <li>• Change parameter: NFS in I2 ADF</li> <li>• Change parameter <math>\sigma_G</math> in I2 ADF (Table 3.4.1.1-II)</li> <li>• Change content of Level 2/res products – GAP</li> <li>• Change time sampling discretisation</li> <li>• Add covariance matrix explanation</li> </ul> <p>Section 5</p> <ul style="list-style-type: none"> <li>• Replace SMO by PFG VER-1/2: Depending on NFS, Apply either a Gaussian filter or a Tikhonov regularization to the vertical inversion matrix</li> <li>• Unit conversion applied on kernel matrix</li> <li>• Suppress VER-3</li> </ul> <p>Section 6</p> <ul style="list-style-type: none"> <li>• GOMOS Atmospheric Profile (GAP): not used in this version</li> <li>• Time sampling in equation (6.5.3.7-73)</li> </ul>
31-MAY-2003	Level 2 version 4.00 at PDHS-E and PDHS-K	<p>Algorithm baseline level 2 DPM 5.4:</p> <ul style="list-style-type: none"> <li>• Revision of some default values</li> <li>• Add a new parameter</li> <li>• Transmission model computation: suppress tests on valid pixels and species</li> <li>• Apply a Gaussian filter to the vertical inversion matrix</li> <li>• Very low signal values are substituted by threshold value</li> </ul>
21-NOV-2002	Level 2 version 3.61 at PDHS-E and PDHS-K	<p>Algorithm baseline level 2 DPM 5.3a:</p> <ul style="list-style-type: none"> <li>• Revision of some default values</li> <li>• Wording of test T11</li> <li>• Dilution term computation of jend</li> <li>• Covariance computation scaling applied before and after</li> </ul>

**Table 6-2: GOPR level 2 product version and main modifications implemented**

Date	Version	Description of changes
14-OCT-2005	GOPR_6.0f	<ul style="list-style-type: none"> <li>• The optimisation of the DOAS iterations</li> <li>• Negative column densities and local densities not flagged anymore</li> <li>• Suppress the setting of maximum error in case of negative local densities</li> <li>• Correction of H RTP discrepancies, and error estimates fixed</li> </ul> <p>Configuration for second reprocessing:</p> <ul style="list-style-type: none"> <li>○ 2<sup>nd</sup> order polynomial for aerosol</li> <li>○ Air fixed to ECMWF (local density set to 0 in the L2 products)</li> <li>○ Orphal cross-sections for O<sub>3</sub></li> <li>○ GOMOS cross-sections for other species</li> <li>○ Covariance matrix terms linked to air set to 0</li> <li>○ Air and NO<sub>2</sub> additional errors set to 0</li> </ul>
17-MAR-2004	GOPR 6.0a	<ul style="list-style-type: none"> <li>• Rename Turbulence MDS into High Resolution Temperature MDS (H RTP)</li> <li>• Add vertical resolution per species in local densities MDS</li> <li>• Add Solar zenith angle at tangent point and at satellite level in</li> </ul>



		<ul style="list-style-type: none"> <li>geolocation ADS</li> <li>Add "tangent point density from external model" in geolocation ADS</li> <li>Suppress contribution of "tangent point density from external model" in "local air density from GOMOS atmospheric profile" in geolocation ADS</li> </ul>
18-AUG-2003	GOPR 5.4d	<ul style="list-style-type: none"> <li>Tikhonov regularisation is implemented</li> </ul>
18-MAR-2003	GOPR 5.4b	<ul style="list-style-type: none"> <li>Modification to implement the computation of Tmodel for spectrometer B (in version 5.4b, the Tmodel for SPB is still set to 1)</li> </ul>
30-JAN-2003	GOPR 5.4a	<ul style="list-style-type: none"> <li>Modifications for ACRI internal use only. No impact on level 2 products.</li> </ul>

### 6.1.2 AUXILIARY DATA FILES (ADF)

The ADF's files in table 6.1-3 and 6.1-4 are used by the PDS to process the data from level 1 to level 2. For every type of file, the validity runs from the start validity time until the start validity time of the following one, but if an ADF file has been disseminated after the start validity time, it is obvious that it will be used by the PDHS-E and PDHS-K PDS only after the dissemination time (this happens the majority of the time). Note that the files outlined in yellow are the set of auxiliary files used during the reporting period.

**Table 6-3: Historic GOM\_PR2\_AX files used by PDS for level 2 products generation. The GOM\_PR2\_AX is a file containing the configuration parameters used for processing from level 1b to level 2 products**

Used by PDS for Level 2 products generation during	GOM_PR2_AX (GOMOS Processing level 2 configuration file)
01-MAR-2002 → 29-JUL-2002	GOM_PR2_AXVIEC20020121_165624_20020101_000000_20200101_000000 <ul style="list-style-type: none"> <li>Pre-launch configuration</li> </ul>
30-JUL-2002 → 02-SEP-2002	GOM_PR2_AXVIEC20020729_083851_20020301_000000_20100101_000000 <ul style="list-style-type: none"> <li>Maximum value of chi2 before a warning flag is raised (set to 5)</li> <li>Maximum number of iterations for the main loop (set to 1)</li> </ul>
03-SEP-2002 → 12-NOV-2003	GOM_PR2_AXVIEC20020902_151029_20020301_000000_20100101_000000 <ul style="list-style-type: none"> <li>Maximum value of chi2 before a warning flag is raised (set to 100)</li> </ul>
13-NOV-2003 → 22-MAR-2004	GOM_PR2_AXVIEC20021112_170458_20020301_000000_20100101_000000 <ul style="list-style-type: none"> <li>Smoothing mode</li> <li>Hanning filter</li> <li>Number of iterations</li> <li>Spectral windows to suppress the O2 absorption in the high spectral range of SPA2</li> </ul>
23-MAR-2004 <i>Note:</i> this file was used by the GOMOS/4.02 processors before the IECF dissemination. The dissemination was done on 25 <sup>th</sup> March 2004	GOM_PR2_AXVIEC20040316_145613_20020301_000000_20100101_000000 <ul style="list-style-type: none"> <li>Pressure at the top of the atmosphere</li> <li>Number of GOMOS sources data (used in GAP)</li> <li>Activation flag for GOMOS sources data (GAP)</li> <li>Smoothing mode (after the spectral inversion)</li> <li>Atmosphere thickness</li> </ul>
08-AUG-2006 Used at the time of switching over GOMOS/5.00	GOM_PR2_AXNIEC20051021_081111_20020301_000000_20100101_000000 <ul style="list-style-type: none"> <li>Several level 2 processing configuration parameters</li> </ul>

**Table 6-4: Historic GOM\_CRS\_AX files used by PDS for level 2 products generation. The GOM\_CRS\_AX is a file containing the cross sections used for processing from level 1b to level 2 products**

Used by PDS for Level 2 products generation during	GOM_CRS_AX (GOMOS Cross Sections file)
01-MAR-2002 → 08-MAR-2002	GOM_CRS_AXVIEC20020121_164026_20020101_000000_20200101_000000 <ul style="list-style-type: none"> <li>• Pre-launch configuration</li> </ul>
09-MAR-2003 → 29-JUL-2002	GOM_CRS_AXVIEC20020308_185417_20020101_000000_20200101_000000 <ul style="list-style-type: none"> <li>• Corrected NUM_DSD in MPH - was 14 and is now 19 - and corrected spare DSD format by replacing last spare by carriage returns in file GOM_CRS_AXVIEC20020121_164026_20020101_000000_20200101_000000</li> </ul>
30-JUL-2002 → 25-MAR-2004	GOM_CRS_AXVIEC20020729_082931_20020301_000000_20100101_000000 <ul style="list-style-type: none"> <li>• O3 cross-sections summary description (SPA)</li> <li>• NO3 cross-sections summary description</li> <li>• O2 transmissions summary description</li> <li>• H2O transmissions summary description</li> <li>• O3 cross sections (SPA)</li> </ul>
26-MAR-2004 <i>Note:</i> the file was disseminated on 27 Jan 2004 but could not be used by PDS until version GOMOS/4.02 was in operation	GOM_CRS_AXVIEC20040127_150241_20020301_000000_20100101_000000 <ul style="list-style-type: none"> <li>• Update of the O2 and H2O transmissions (S.A input)</li> <li>• Extension by continuity of the O3 cross-section for SPB</li> </ul>
08-AUG-2006 Used at the time of switching over GOMOS/5.00	<b>GOM_CRS_AXNIEC20051021_080452_20020301_000000_20100101_000000</b> <ul style="list-style-type: none"> <li>• Updated O<sub>3</sub> cross-sections</li> </ul>

### 6.1.3 RE-PROCESSING STATUS

The improvement of the GOMOS processing chain is a continuous on-going activity, not only for the processing algorithm but also for the instrument characterization data. In order to provide the best quality products to the users and due to the normal delay between algorithm specification and implementation in the operational PDS, it was decided to reprocess the GOMOS data using the Gopr prototype.

The second reprocessing activity covering years 2002-2006 (until 4<sup>th</sup> July 2006) using the prototype Gopr\_6.0c\_6.0f is completed. All reprocessed data can be retrieved via web query from <http://www.enviport.org/gomos/index.jsp>. FTP access to bulk reprocessing results (one tar file of GOMOS products per day) is allowed from the D-PAC: <ftp://gomo2usr@ftp-ops.de.envisat.esa.int>. See more details and latest status on [http://www.enviport.org/boards/board\\_gomos.htm](http://www.enviport.org/boards/board_gomos.htm)

## 6.2 Quality Flags Monitoring

In this section, some information contained in the Quality Summary data set of the level 2 products arrived during reporting period is shown. In particular, the percentage of flagged points per profile for the local species O<sub>3</sub>, H<sub>2</sub>O, NO<sub>2</sub> and NO<sub>3</sub> is depicted. Only products in dark limb illumination conditions and without fatal errors (error flag in the MPH set to "0") are used.

The flagging strategy for GOMOS version GOMOS/5.00 foresees that a profile point is flagged when:

- The local density is greater than a given maximum value
- The line density is not valid. And it occurs when:
  - The acquisition from level 1b is not valid
  - There is no acquisition used for reference star spectrum
  - The line density is greater than a given maximum value

Only for species: air, aerosol, O<sub>3</sub>, NO<sub>2</sub>, NO<sub>3</sub>, OClO

- No convergence after a given number of LMA iterations
- $\chi^2$  out of LMA is bigger than  $\chi^2$
- Failure of inversion

Only for species: O<sub>2</sub>, H<sub>2</sub>O

- Spectro B only: no convergence
- Spectro B only: data not available
- Spectro B only: covariance not available

There are points mainly between -85° and 15° latitude (fig. 6.2-1) because in this period of the year full dark illumination condition occultations (only those products have been used for these plots) are geolocated on that region. In summer, full dark illumination data are mainly in the Southern Hemisphere while in winter it is the contrary: full dark illumination occultations are found mainly in the Northern Hemisphere.

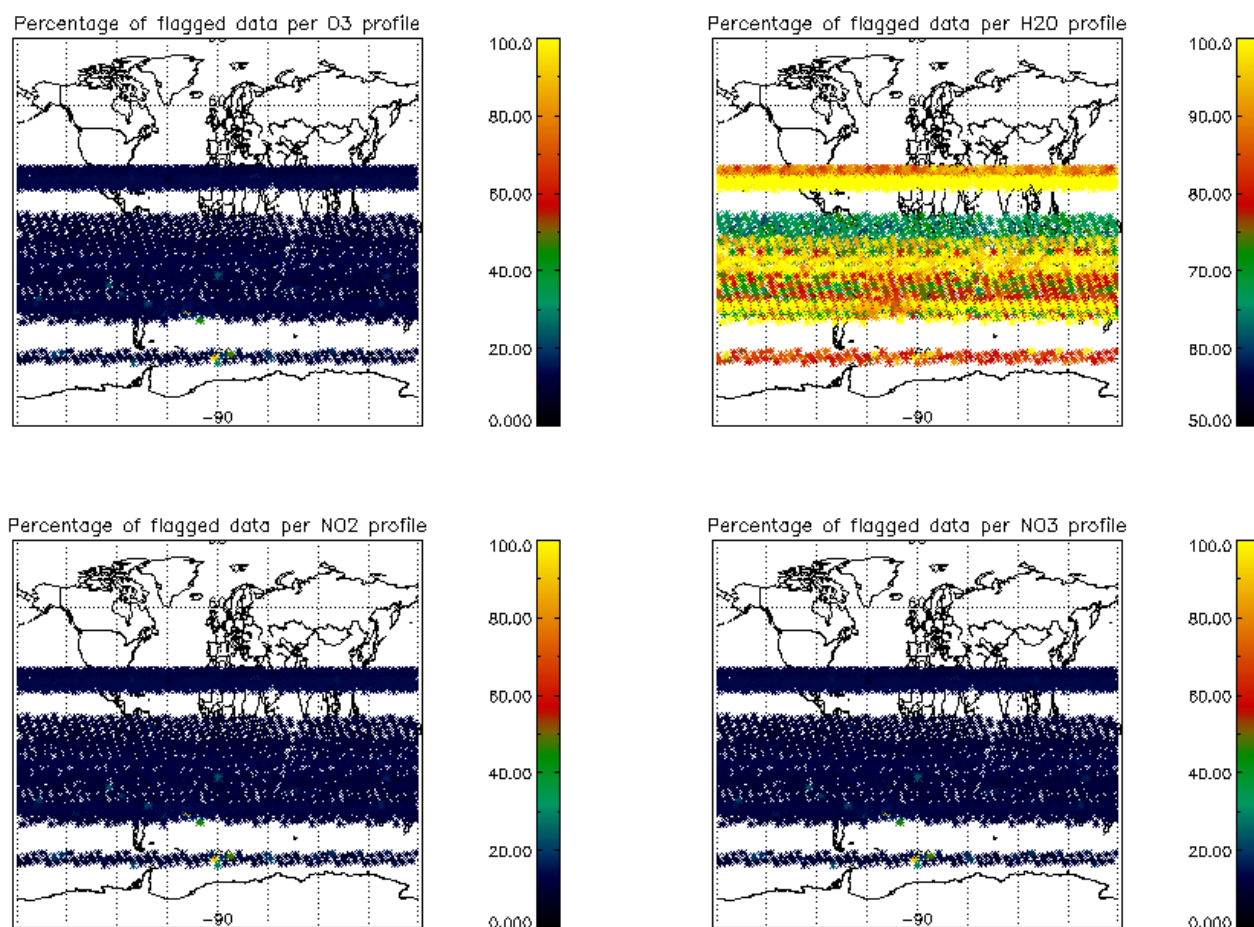


Figure 6.2-1: Percentage of flagged points per profile

Looking at fig. 6.2-1, the most evident characteristic that can be observed is the high percentage of flagged points per profile for some H<sub>2</sub>O profiles. Users should be careful in using these data as the quality is only guaranteed for few stars. As a consequence of the new flagging strategy the percentage of flagged points per profile for O<sub>3</sub>, NO<sub>2</sub> and NO<sub>3</sub> is around 10-15%. It can be seen also that there are latitudinal bands with almost the same color (same percentages) mainly for H<sub>2</sub>O. This means that the percentages of flagged points per profile have a dependence on the stars that have been observed: a given star is always observed at the same latitude but at different longitude.

### 6.3 Other Level 2 Performance Issues

#### 6.3.1 MONTHLY OZONE AVERAGE

The plot presented in fig. 6.3-1 is the average of the Ozone values during the reporting month in a grid of 0.5 degrees in latitude per 1 km in altitude. Only occultations in dark limb have been used.

At low latitudes and at 20-35 km altitude range the plot is spoiled with high values that are not real. The principal reason of the ozone quality degradation is the increase of DC.

Even though there is a reduction on latitude coverage due to the restricted azimuth field of view of the instrument, still some known characteristics can be seen:

- O<sub>3</sub> concentrations show a decrease with latitude near 40 km altitude. In the lower latitudes O<sub>3</sub> is generated by photolysis of O<sub>2</sub>
- In the middle stratosphere (25-30 km) O<sub>3</sub> is strongly influenced by transport effects. Strong meridional and zonal transport is visible in middle and higher latitudes
- The lower stratosphere shows an O<sub>3</sub> increase with latitude. Highest values can be found within higher latitude regions due to downward transport of rich air masses

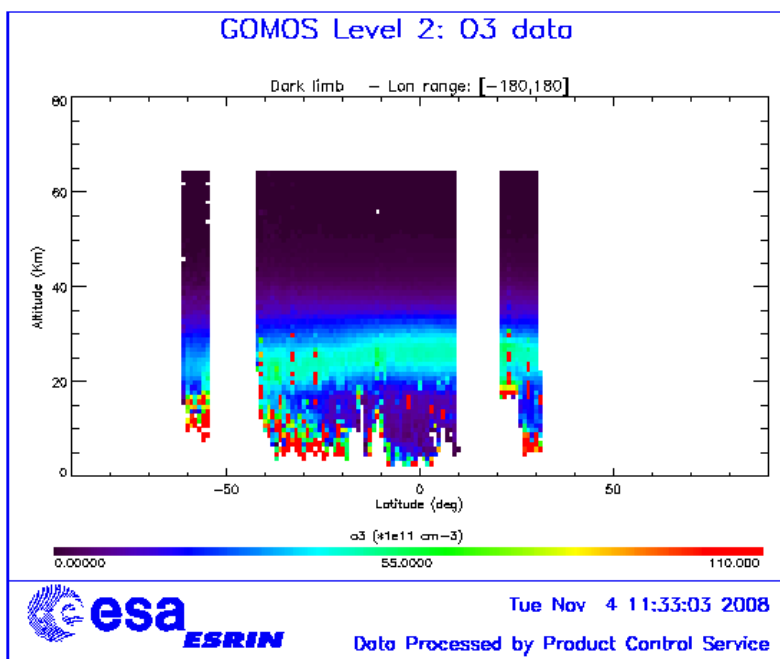


Figure 6.3-1: Average GOMOS O<sub>3</sub> profile during the reporting month: average in a grid of 0.5° latitude x 1 km altitude

### 6.3.2 OZONE DISPERSION MONITORING

This section is the output of a QWG request for the monitoring of the dispersion around the equator [-30°, 30°] using the brightest star of the day and with temperature greater or equal than 7000 k. This request includes the plot of daily averaged ozone, daily averaged  $\chi^2$ , daily averaged estimated errors and daily dispersion (defined as STD/Mean in %). The first step is the interpolation to given altitude layers (20, 25, 30, 40, 50, 60, 70, 80 and 90 km) and afterwards the daily average is performed. More than 5 profiles per day should be used for the average, if for a given day the number of profiles is less than 5 (for the brightest star) then the following star in increasing magnitude is chosen.

Fig. 6.3-2 shows the daily ozone average for the reporting month. The numbers below the lower curve are the star ID of the stars used for the daily averages whilst the numbers above the upper curve are the number of profiles used for every daily average. As expected, the curves at 20 and 80 km show more “instability” due to processor limitations. In fact, data below 20 and above 60 km should be taken with care.

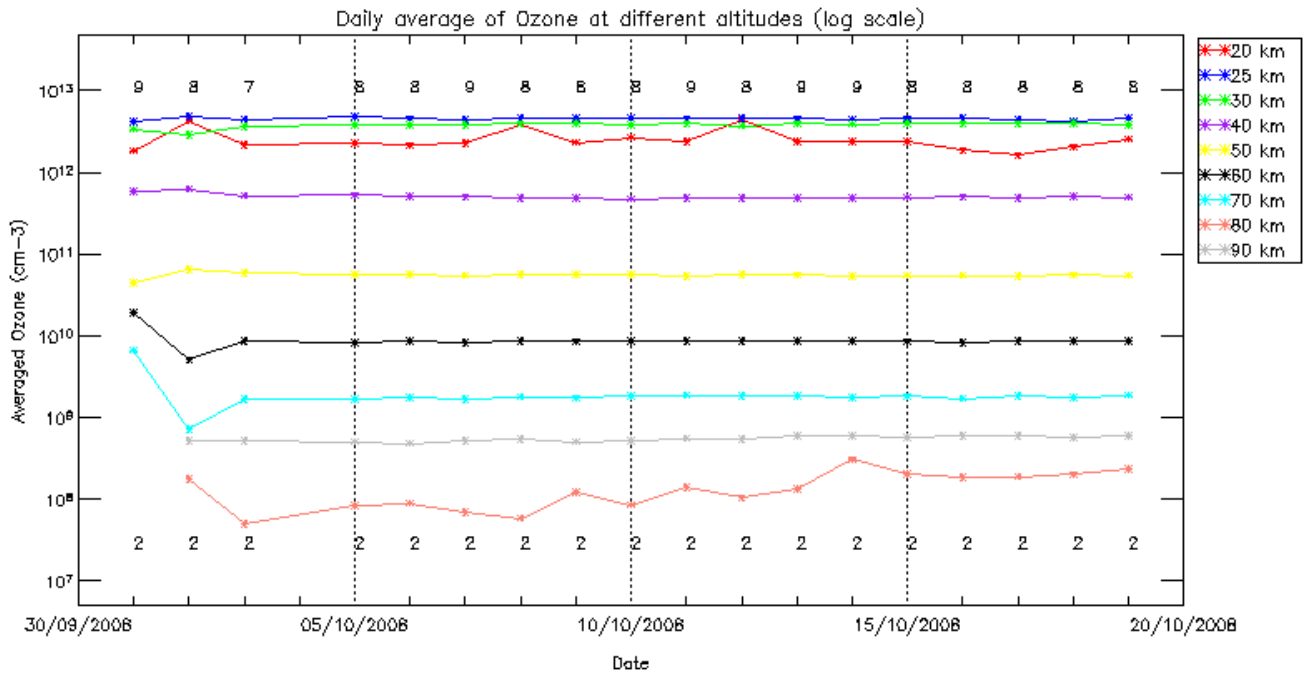


Figure 6.3-2: Daily ozone average at different altitude layers for the reporting month

The daily averaged  $\chi^2$  (fig. 6.3-3) shows some variability even if the data above the SAA have not been used. Also fig 6.3-4 and 6.3-5 show a variability that was not expected by the members of the QWG.

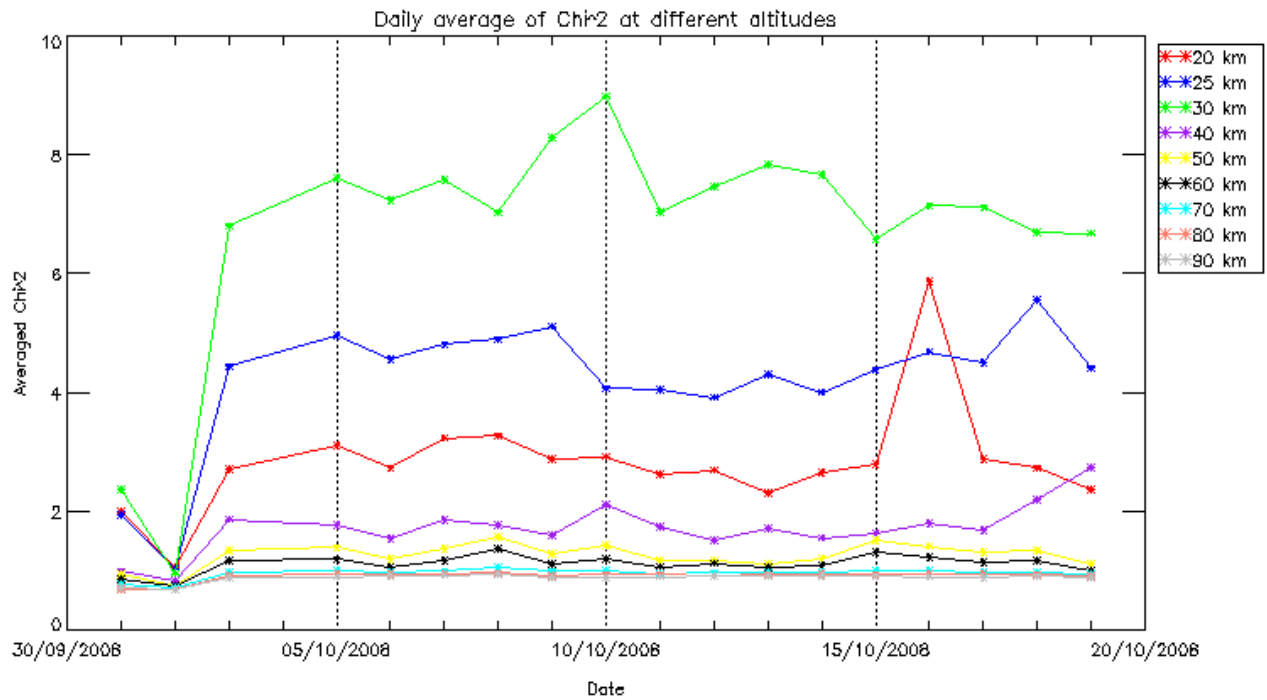


Figure 6.3-3: Daily chi2 average at different altitude layers for the reporting month

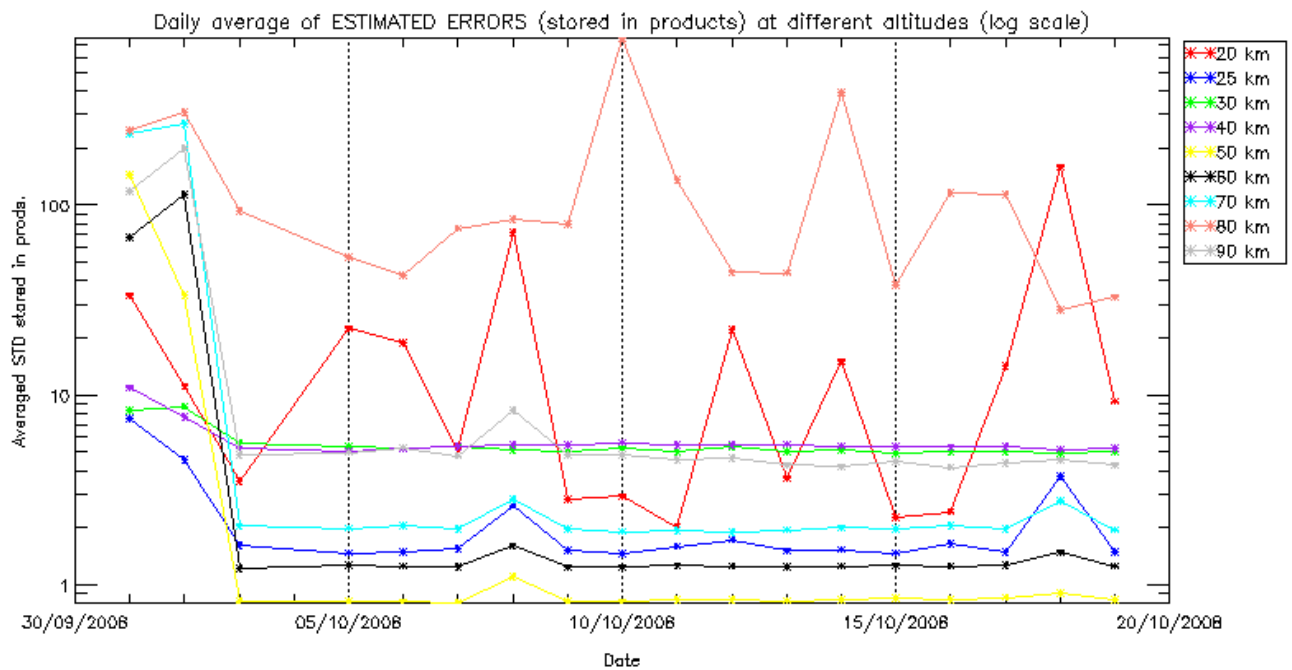


Figure 6.3-4: Daily average of the estimated errors at different altitudes

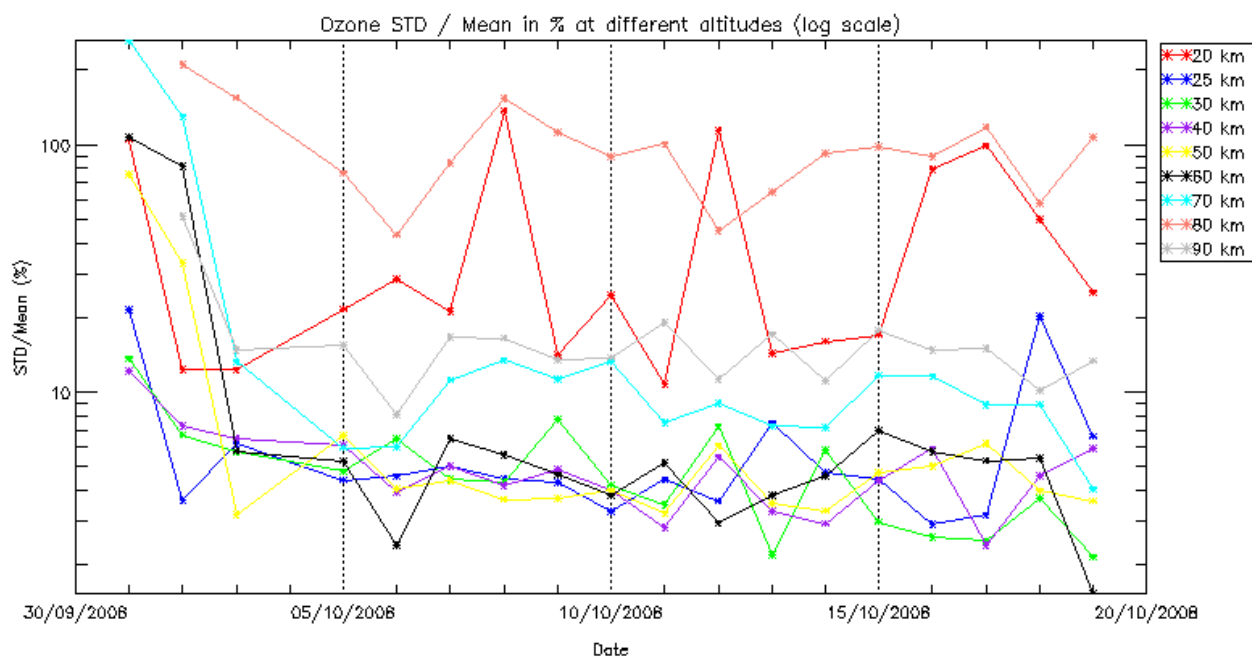


Figure 6.3-5: Daily dispersion defined as STD/Mean in %

## 7 VALIDATION ACTIVITIES AND RESULTS

### 7.1 GOMOS-ECMWF Comparisons (Rossana Dragani, ECMWF input)

The full ECMWF validation report is available at the following link:

[http://earth.esa.int/pcs/envisat/calval\\_res/2008/ecmwf\\_gomos\\_monthly\\_200810\\_all.pdf](http://earth.esa.int/pcs/envisat/calval_res/2008/ecmwf_gomos_monthly_200810_all.pdf)

A summary of the report is reported in the following paragraph:

- There were no data in the BUFR files at high latitudes in the NH.
- Overall the temperature in the GOMOS BUFR files was found in good agreement with the ECMWF temperature. Both the global mean and area averaged first guess and analysis departures were typically negative at all levels in the global average with values of less than -2K in the lower stratosphere, and up to -8K in the upper stratosphere and mesosphere.
- The quality of the GOMOS ozone profiles was much improved compared with that in September. In the global mean, the departures between GOMOS and ECMWF ozone profiles were within -3 and +10% in most of the stratosphere and mesosphere, but larger than 50% at some layers in the lower stratosphere. When averaging over latitudinal bands, the first guess and analysis departures between the GOMOS ozone profiles and their model equivalent were typically within -10 and +15% in most of the stratosphere and mesosphere in the tropics and at mid-latitudes in the NH, but larger departures were found at mid and high latitudes in the SH. The standard deviations of the analysis and first guess departures were larger than 10% at all latitudes and levels.
- The quality of the water vapour retrievals was still quite poor despite the data used in the monitoring statistics were only those acquired in dark-limb conditions. The monitoring statistics showed that the GOMOS water vapour values were from one to four orders of magnitude larger than their model equivalent at all vertical levels and latitudes. The largest differences between

GOMOS WV and ECMWF WV were still found in the Stratosphere. A slightly higher level of agreement between the GOMOS WV data and their model equivalent was found at high latitudes in the SH.

- At some levels and latitudinal bands, the number of GOMOS water vapour observations was too low to be statistically significant.
- The monitoring statistics for October were produced with the operational ECMWF model, CY33R2.

## 7.2 Comparison of ozone and temperature profiles with lidar data - Satellite validation with lidar (VALID) (A. van Gijssel, RIVM, QWG input).

The following analysis compares the GOMOS ozone density number with that measured by lidar systems contributing to the VALID project. Both datasets (covering the period 2002-2007) have been restricted to a collocation difference of a maximum of 800 km and 20 hours and a maximum error of 30%. Furthermore, the GOMOS profiles are required to be taken in ‘dark limb’ mode and ozone number density values have to range between 0 and  $10^{19}$  molecules/m<sup>3</sup>.

The plots of fig. 7.2-1 illustrate the results of the comparison between ozone number density estimated by GOMOS and the collocated lidars (“VALID”). The left panel shows the mean (thick lines) of the VALID lidars (blue) and the GOMOS (red) ozone profiles together with the respective standard deviations (thin lines). In the middle panel, the mean (green) and median (black) of the relative differences between GOMOS and VALID are shown, together with the range indicated by the mean ± one standard deviation (thin green lines) and the mean ± two standard errors (thin grey lines), are shown. On the right side of the middle panel the number of collocations for each altitude is listed. The right panel shows the standard deviations of GOMOS (red), VALID (blue) and the standard deviation of the differences between GOMOS and VALID (green) as a function of altitude.

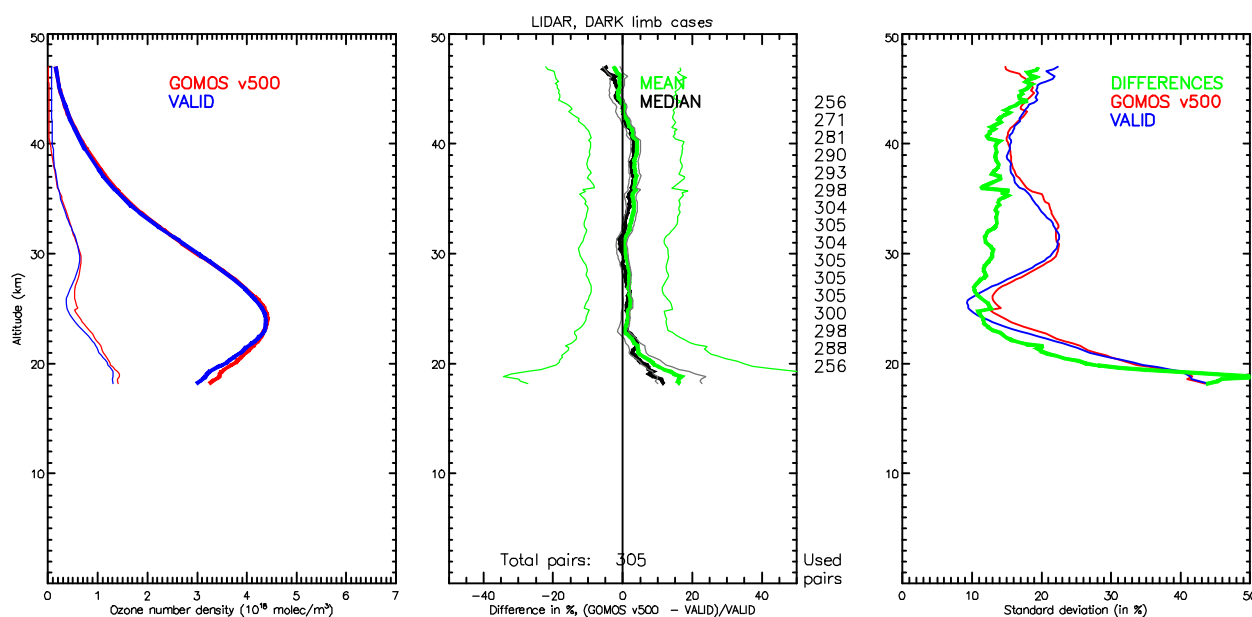
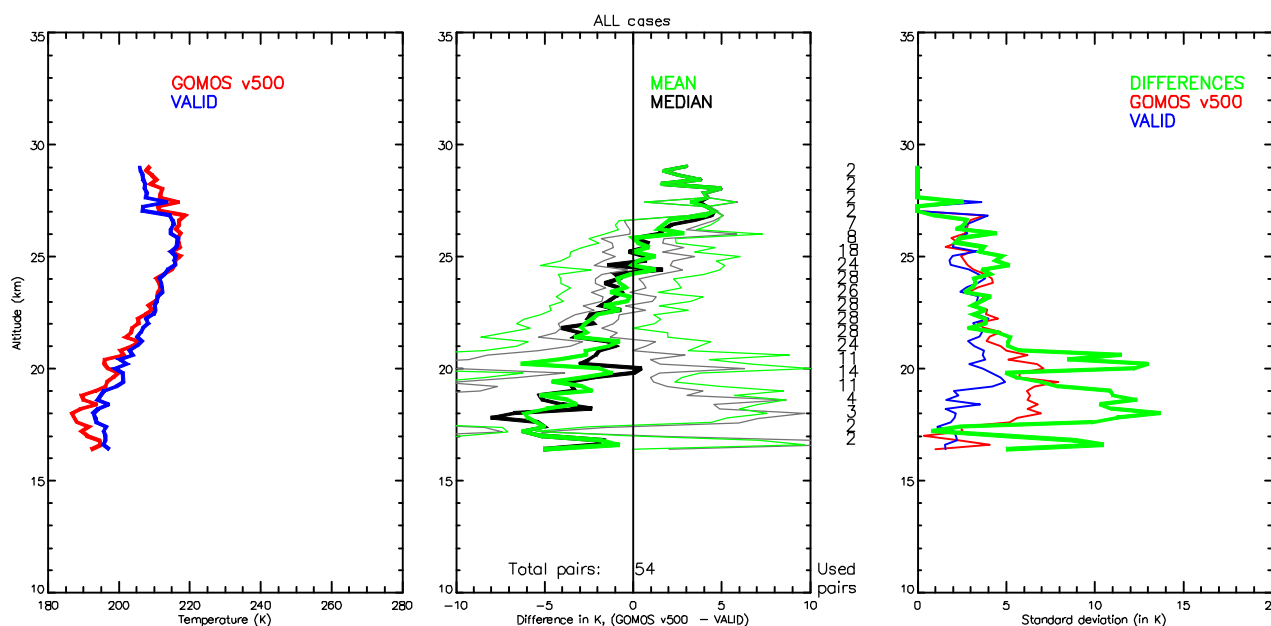


Figure 7.2-1: Comparison between ozone number density estimated by GOMOS and the collocated lidars (“VALID”)



In general, the ozone profiles provided from GOMOS version 5.00, match very well with those originating from the lidar measurements. Some outliers still exist, which are especially visible at the lower part of the profile where the mean deviates from the median (middle plot). In this altitude region, the GOMOS ozone profiles also significantly differ from the lidar measurements with an overestimation of the ozone concentration by GOMOS.

The second series of figures illustrates the comparison between the GOMOS high resolution temperature profiles (HRTP) obtained in ‘dark limb’ mode and the T profiles measured by lidar and balloon sondes.



**Figure 7.2-2: Comparison of lidar/balloon sonde (‘VALID’) versus GOMOS v5.00 temperatures as given by the HRTP algorithm**

The fig. 7.2-2 shows the comparison of lidar/balloon sonde (‘VALID’) versus GOMOS v5.00 temperatures as given by the HRTP algorithm. The left panel shows the mean of the VALID (blue) and the GOMOS (red) temperature profiles. In the middle panel, the mean (green) and median (black) of the differences between GOMOS and VALID are shown, together with the range indicated by the mean  $\pm$  one standard deviation (thin green lines) and the mean  $\pm$  two standard errors (thin grey lines). On the right side of the middle panel is listed the number of collocations for each altitude. The right panel shows the standard deviations of GOMOS (red), VALID (blue) and the standard deviation of the differences between GOMOS and VALID (green) as a function of altitude.

Despite the non-strict collocation criteria (5 hours and 500 km), very few collocations were available. This analysis should be therefore considered preliminary because of the low number of collocations (maximum of 28 collocations at any altitude). This is partially due to the HRTP algorithm still being under development and thus the product is not always available. Nevertheless, agreement is generally good (within the  $2 \times$  standard error range), especially for the mid-part of the profiles. Although the number of collocations is not significant at the top and bottom of the profiles, an overestimation is seen at the top with an underestimation by GOMOS at the lower parts of the profile.

It is foreseen that a new HRTP algorithm will be implemented in the next version of the IPF. This HRTP algorithm will take into account some modifications tested and specified in the frame of a specific

project. The prototype algorithm developed for this project has shown very promising results, and a strong improvement of the H RTP quality is expected with the new processing.